8-2005

Evaluation of Experimental Bridge: Massman Drive Bridge Over Interstate 40 in Davidson County

Jeremy Glen Pettus
University of Tennessee - Knoxville

To the Graduate Council:

I am submitting herewith a thesis written by Jeremy Glen Pettus entitled "Evaluation of Experimental Bridge: Massman Drive Bridge Over Interstate 40 in Davidson County." I have examined the final electronic copy of this thesis for form and content and recommend that it be accepted in partial fulfillment of the requirements for the degree of Master of Science, with a major in Civil Engineering.

Edwin G. Burdette, Major Professor

We have read this thesis and recommend its acceptance:

James H. Deatherage, David W. Goodpasture

Accepted for the Council:
Carolyn R. Hodges

Vice Provost and Dean of the Graduate School

(Original signatures are on file with official student records.)

To the Graduate Council:

I am submitting herewith a thesis written by Jeremy Glen Pettus entitled "Evaluation of Experimental Bridge: Massman Drive Bridge over Interstate 40 in Davidson County." I have examined the final electronic copy of this thesis for form and content and recommend that it be accepted in partial fulfillment of the requirements for the degree of Master of Science, with a major in Civil Engineering.

Edwin G. Burdette
Edwin G. Burdette, Major Professor

We have read this thesis and
recommend its acceptance:

James H. Deatherage

David W. Goodpasture

Accepted for the Council:

Anne Mayhew
Vice Chancellor and
Dean of the Graduate School

(Original signatures are on file with official student records.)

EVALUATION OF EXPERIMENTAL BRIDGE: MASSMAN DRIVE BRIDGE OVER INTERSTATE 40 IN DAVIDSON COUNTY

A Thesis
Presented for the
Master of Science
Degree
The University of Tennessee, Knoxville

Jeremy Glen Pettus
August 2005

Acknowledgments

I owe credit for completion of my M.S. degree to countless people. I am very thankful for the help because I could not have completed it alone.

The research team and I are thankful to the Tennessee Department of Transportation for its continued support of bridge research. Research is crucial for advancement of bridge technology and to the academic process.

I want to thank Dr. Edwin G. Burdette for his support and guidance over the years. In particular, I am thankful for the time and advice he gave a complete stranger during the Fall of 1998. After I spoke with Dr. Burdette during an impromptu meeting, I made the decision to change majors from physics to civil engineering. It has been the best decision of my academic career. Dr. Burdette's ability as an engineer and professor is widely known, and I am very proud to have been one of his students. He and I both know that my B.S. and M.S. degrees in civil engineering would not have been possible without his guidance and support.

I want to thank Dr. David W. Goodpasture for his efforts with the data acquisition for the project and for serving on my thesis committee. The data quality certainly

made the data analysis less cumbersome and much more enjoyable.

I want to thank Dr. J. Harold Deatherage for serving on my thesis committee and his guidance throughout my undergraduate and graduate career. I have great respect for his academic, business, and engineering philosophy, and like many others, I always welcome his advice.

I want to thank David P. Chapman for his hard work and leadership on the Massman Drive Bridge project. The project has been a real success from start to finish. The photographs in this thesis were taken from his photographic record of the project.

Allison Sharp Pettus, my wife, has been heroic for all of her hard work over the past several years. Unfortunately, her work goes primarily unnoticed by everyone except for Abbey Katelyn Pettus (our daughter) and me.

I want to thank my parents, Ricky G. and L. Gwen Pettus, for their support. They provided encouragement and always knew that I would succeed in my pursuits. I also want to thank my paternal grandparents, Wiley C. and M. Nell Pettus, and my maternal grandparents, Gene and Winda F. Norwood. My family has been a great role model. Among

many things, they have shown me the necessity to work hard at every aspect of life.

Lastly, I want to thank the University of Tennessee for allowing me the opportunity to make my academic dreams a reality. I truly believe that this is a special place, and I will work diligently to make you proud. Thanks for everything; I can truly say, "…Rocky top you'll always be home sweet home to me…" (Bryant 1967)!

Abstract

The Massman Drive Bridge is a 284ft. two-span continuous steel bridge over Interstate 40 in Nashville, TN. The bridge is an experimental design that unifies the construction economy of simple span bridges and the structural economy of continuous span bridges. The structural system involves bridge girders initially erected with simple supports at the center bent and abutments. Before the deck is placed, an experimental connection is used to rigidly connect the two adjacent girders over the center bent. The experimental connection couples a cover plate in tension and two kicker wedge plates in compression. The kicker wedge plates supply resistance with direct bearing between each other and the compression flanges of the adjacent girders.

A total of 84 weldable strain gages were applied to three of the five bridge girders. The majority of the strain gages were placed at the connection on the plates and girder. Data collected during placement of the bridge deck concrete was used to evaluate the bridge performance under dead load. Several live load tests were later performed and will be reported by others.

The data indicate that the three girders instrumented were continuous across the experimental connection. The two interior girders were found to exhibit similar behavior. However, the one instrumented exterior girder was found to have a reduced stiffness at the connection, as compared to the two interior girders. The effectiveness of the connection appears to be dependent on the erection of the wedge plates. A rationale for this behavior is presented but is not conclusive. Overall, the conclusion is drawn that the method works, in the sense that continuity over the center bent was achieved under the weight of the freshly cast deck.

Table of Contents

List of Tables

List of Figures

1. INTRODUCTION

1.1. Background

A research contract between the Tennessee Department of Transportation (TDOT) and The University of Tennessee was executed March 1, 2002, to conduct research on an experimental bridge in Nashville, TN. The subject Massman Drive Bridge (No. 19I00400119) is a replacement to the 220ft. original four-span prestressed concrete bridge (No. 19-04951-1.45). The center bent of the old bridge is retained and incorporated into the center bent of the new bridge, with an additional foundation and column to the east and west. The two-lane bridge bears S14°11'39"E from the north abutment and intersects Interstate 40 near mile marker 214. The new two-span Massman Drive Bridge has a total bridge deck length of 287ft. The distance between bearing centerlines at the abutments is 284ft. with 138.5ft. and 145.5ft. spans to the north and south, respectively. It is constructed of built-up steel girders that act compositely with the reinforced concrete bridge deck.

The bridge is designed to have efficiency advantages over other bridge types. These efficiencies include a decrease in construction time and an increase in structural

performance. During construction, the steel girders are designed to act as simple spans under their self-weight until the connection is made at the center bent. After the connection is made, the girders are designed to act continuously across the center bent with simple supports at the abutments. After construction is complete, the steel girders are designed to act compositely with the concrete deck, be continuous across the center bent, and have semi-rigid connections at the integral abutments. Weldable strain gages were attached to the steel girders at locations of interest. The majority of the gages were concentrated in the area of the connection, which is the region of primary interest. The remainder of the strain gages were placed near midspan and near the abutment.

2. LITERATURE REVIEW

The Massman Drive Bridge is an experimental bridge that is designed to unify the construction economy of simple span bridges and the structural economy of continuous span bridges. This process is accomplished with the application of an experimental connection that rigidly connects two adjacent girders with a cover plate in tension coupled with two kicker wedge plates developing compression. It is the intent of this thesis to investigate the behavior of the connection and evaluate its performance.

The connection has previously been installed on one other bridge in the state of Tennessee, the DuPont Access Bridge in Humphreys County. The two-span bridge has six girder lines with north and south spans of 76ft. and 87ft., respectively. The bridge girders are 33 x 240 wide flange sections of A709 Grade 50W steel. The DuPont Access Bridge differs from the Massman Drive Bridge in that the abutments were integral with the girders during the dead load test. It was found that the experimental connection provided continuity across the center support in the three girders tested (Burdette et al 2004).

The Nebraska Department of Roads has sponsored a study involving a construction technique that is similar to the Massman Drive Bridge in some regards. In their study, the girders are erected as simple spans; plates are attached to the bottom flanges and are connected across the pier with a partial penetration weld. The connection of the top flange of the girders is achieved through the reinforced concrete of the deck and diaphragm. As a result, the bridge behaves as simple spans under the dead load of the deck, and after the deck has cured, the bridge behaves with continuity across the center bent under additional dead and live loads. Full-scale model tests are complete, and field testing of an experimental bridge is underway in Omaha, NE (Azizinamini 2004).

The experimental connection for the Massman Drive Bridge uses a lap splice for the top cover plate in tension and an unbolted bearing type connection in compression. Slip critical connections have evolved over several decades in proportion to the increased use of high-strength bolts instead of rivets (Salmon and Johnson 1996). The slip critical connection has been found to be highly dependent upon the slip coefficient of the faying surfaces and the bolt tension. However, the ultimate strength of the slip

critical connection usually depends upon such factors as bolt shear strength and material rupture strength (Kulak et al 2001).

There does not appear to be literature addressing plates that are in direct bearing as seen in the experimental connection for Massman Drive Bridge. Work has been done with regard to bolts bearing against plates, but the applicability is certainly limited.

3. DESCRIPTION OF THE MASSMAN DRIVE BRIDGE

3.1. Substructure

The Massman Drive Bridge is a two span continuous bridge with a 284ft. total length. The north and south abutments serve as simple supports for the girders during most of the construction. After the bridge deck pour sequence, the girder supports at the abutments act integrally with the girders. After the parapet construction and during actual service of the bridge, the integral abutments have been designed to behave as semi-rigid supports for the girders. The center bent is a simple support for the girders during erection, construction, and service of the bridge.

Each of the reinforced concrete abutments are supported with twelve HP10x42 piles. Each of the abutment piles were to be driven to refusal or have a minimum bearing of 55 tons.

The center bent from the old bridge consisted of a bent cap spanning between two columns with spread footing foundations. One additional column and foundation was constructed on each side of the old bent cap. The column foundation constructed on the west side consisted of a pile cap and seven HP10x42 piles driven to refusal. The east

column foundation consisted of a rock bearing footing. Some concrete of the old bent cap was removed to allow mechanical anchorage to the longitudinal steel of the new bent cap. TDOT plans and specifications for the Massman Drive Bridge may be consulted for further detailed information.

3.2. Superstructure

The Massman Drive Bridge girders are built-up with $1\frac{1}{2}$ x 18in. flanges continuously welded to the $\frac{5}{8}$ x 60in. web (A709 Grade 50W). Web stiffeners of $\frac{7}{8}$ x $8\frac{1}{2}$in. (at supports) and $\frac{7}{8}$ x 7in. (interior) are spaced at 25ft. along both sides of the web. The web stiffeners are omitted from the exterior face of the two exterior girders. The connection of the two girders where they meet at the center bent has $\frac{1}{2}$ x $19\frac{1}{2}$ x 57in. plates continuously welded with a $\frac{5}{16}$in. weld to the bottom of the bottom flange. Lateral cross brace trusses of 4 x 4 x $\frac{1}{2}$in. angles are attached at 25ft. centers to the web stiffeners at all locations along the girders except at the center bent. Bracing at the

center bent is provided by two 15 x 33.9 channels during construction, and a reinforced concrete diaphragm is placed monolithically with the bridge deck. A plan and elevation drawing provided by the Tennessee Department of Transportation (TDOT) has been reproduced and is shown as Figure A1 in the Appendix.

The connection of the north and south girders across the center bent is provided with a 2 x 18 x 126in. cover plate for the tension element and two 2 x 6± x $23\frac{1}{2}$in. kicker wedge plates for the compression element. The cover plate is a slip critical connection with 72, 1in. diameter A490 Grade 50W bolts on each end. The kicker wedge plates are driven together in opposing directions to achieve bearing against each other and against the bottom flange of the girders. The kicker wedge plates and the bottom flanges of the girders are welded with a $\frac{1}{4}$in. weld. An elevation schematic of this connection is shown as Figure A2. A plan schematic of the top cover plate and bottom cover plate/kicker wedge plates are shown as Figures A3 and A4, respectively.

Shear studs $\frac{7}{8}$ x $6\frac{3}{4}$in. were field installed at locations of positive moment in the girders. The longitudinal stud spacing varied from 7in. to 21in., with the closer spacings being located near the inflection points. The studs are in groups of three, with one stud spaced at $3\frac{1}{2}$in. on each side of the stud centered over the web. Composite behavior of the girders with low strength concrete is discussed further in Section 5.3. The TDOT plans and specifications for Massman Drive Bridge may be referenced for more specific and detailed design information.

4. DATA COLLECTION

4.1. Girder and Strain Gage Descriptors

The Massman Drive Bridge over Interstate 40 in Nashville, Tennessee has five steel girders. The south girders are numbered ascending from east to west with the first girder being girder 2 (i.e. from east to west the girders are numbered 2, 3, 4, 5, and 6). Strain gages were placed on the south span girders 4, 5, and 6 at eight stations along each of the girders. At each station, strain gages were placed at different stages that are dependent on the data needed for each particular station. A total of 28 strain gages were placed on each of the three girders. All of the 84 strain gages have a unique and codified number that reveals the gage location. The strain gage coding system is described in detail below.

- The first of the three digits represents the girder number on which the gage is located. For instance, all gages on girder 4 are of the form 'gage 4XX'. Table A1 describes the girder designations in more detail.
- Each of the three girders had eight stations that were of interest in this study. The second digit of the strain gage number designates the station at which the

gage is located. They are numbered in ascending order from north to south. The stations begin with station 1 at the center bent and end with station 8 near the south abutment. For example, all gages at station 3 are located 1.5ft. from the connection centerline and are of the form 'gage X3X'. Table A2 describes the station designations in more detail.

- Each of the eight stations has from 1 to 7 gages located at different stages. The stages begin with stage 1 and 2 and end with stage 6 and/or 7. Stages 1 and 2 are for gages located on the top cover plates. These gages are centered between the two lines of bolts on each side of the web. Stage 6 is typically on the top of the bottom flange, with the exception being the gages located at station 1. At this station, gages X16 and X17 are located on top of the kicker wedge plates as close to the weld as possible. A typical example is for all of the strain gages located on the top cover plate. These gages are at either stage 1 or 2 and are of the form 'gage XX1 or XX2'. Table A3 describes the stage designations in more detail.

Figure A5 shows a cross section of the Massman Drive Bridge and the numbering system for the girders. Figure A6 shows an elevation view along girder 4 with the strain gage locations labeled. Girders 5 and 6 follow the same numbering code; again, the first digit corresponds to the particular girder number.

4.2. Strain Gages and Data Collection Equipment

The gages used on Massman Drive Bridge are weldable strain gages purchased from HITEC PRODUCTS, INC. in Ayer, MA. These gages are bonded to a stainless steel shim, prewired, and waterproofed. The three different strain gages used are listed below.

- HBW-35-500-6-10VR $\frac{1}{2}$in. strain gage with 10ft lead wire
- HBW-35-500-6-5VR $\frac{1}{2}$in. strain gage with 5ft lead wire
- HBW-35-250-6-5VR $\frac{1}{4}$in. strain gage with 5ft lead wire

The strain gages used have a base resistance of 350 Ohms and a typical gage factor of 2.005±. Before application, the base steel was removed of paint and/or rust and was ground smooth. Approximately 50% of the strain gages were installed using a Vishay Micro-Measurements Portable Strain Gage Welding/Soldering Unit Model 700. The remainder were

installed using a HITEC PRODUCTS, INC. HW-1 Portable Spot Welder. The HITEC welder was originally used until a malfunction rendered it inoperable. At that point, the HITEC welder was repaired and used intermittently while the Vishay welder was primarily used. Visual inspection reveals that the weld quality of the two welders is almost identical. In terms of function, the HITEC welder is more productive, but the Vishay welder is much easier to operate. The strain gages were welded to the girders in a uniform fashion along each flank of the strain gage. Spot welds were typically placed at an approximate center-to-center spacing of 0.06in. in a zigzag pattern. In difficult to access locations, the weld placement was not as symmetric as the welds at locations with easy access.

The strain gages are delivered with wire lengths on the order of 5ft. Additional three-wire cable was used to extend the strain gage wires to the desired length. After the wires were spliced and soldered, the majority of the wire lengths were approximately 200ft. in length. The strain gage wires were routed along the length of the girder through a small opening between the bottom flange, web, and web stiffener. The wires were fastened to the

girder with a combination of these anchor points and duct tape.

The data collection hardware was housed in an office trailer located on the west side of the south abutment. The hardware consisted of an OPTIM MEGADAC 3415AC interfaced through a GPIB/IEEE-488 to a Dell Latitude Notebook. The primary software consisted of TCS Version 3.4.0 and Microsoft Windows 2000 Professional.

Photographs of the bridge during different phases of construction and instrumentation are shown as Figures A7 through A10.

5. CONNECTION CONTINUITY

5.1. Description of Dead Load Test

The dead load test objective was to determine if there is continuity through the connection over the center bent. The dead load test involved a uniform load application, but the researchers had little control over the rate at which the load was applied.

The data acquisition system was programmed to sample at a rate of 0.2 scans/second (i.e. 1 sample per 5 seconds). The strain gages were balanced before the beginning of concrete placement. Data were acquired continuously during the two day concrete placement operation. The bridge deck concrete placement was partitioned into 5 phases. The pouring sequence is shown in the design plans provided by TDOT and is reproduced here in Figure A11. A total of 368yd^3 of concrete was placed over an area of 13,202ft^2 (i.e. 46 x 287ft.). With reference to Figure A11, it should be noted that a 5ft. length of deck is included during the pour of each integral abutment. Phase 1 of the deck placement was started on January 4, 2005 at 8:51a.m. EST and ended at 11:55a.m. EST. There was one significant disruption in placement that lasted from approximately 9:05a.m. EST to 9:35a.m. EST.

Phase 2 of the placement began at 1:15p.m. EST and ended at 3:07p.m. EST. The following day, January 5, 2005, pouring of the reinforced concrete diaphragms was conducted between 11:04a.m. and 11:09a.m. EST. At 11:10a.m. EST, phase 3 of the deck pour began and was completed at 2:07p.m. EST. On day 2 there were no noticeable interruptions.

The composite behavior of girders with 1-day old concrete was not initially known. For this reason, notes and deflection data were recorded with the intent to perform a parametric study to determine if composite action was apparent. The following list shows discreet points in time that serve as control points for data collection and analysis purposes.

- Time 0 – 8:51a.m. EST (Before the test began.)
- Time 1 – 12:01p.m. EST (After the completion of phase 1 and before the beginning of phase 2.)
- Time 1.5 – 1:30p.m. EST (After the completion of phase 1 and with phase 2 33% complete. Phase 2 began on the north abutment of the bridge and had progressed 28ft. from the construction joint.)

- Time 2 – 11:00p.m. EST (After the completion of phases 1 and 2)
- Time 3 – 2:12p.m. EST (At the completion of phase 3)

5.2. Data

A total of 84 weldable strain gages were installed on the three girders. Before the test date, some gages were found to display large amounts of noise or were inoperable. These strain gages were not monitored during the dead load test. The total number of usable strain gages was 79. The two day test produced a total of 21,955 data points per gage. Review of the data shows evidence that some of the strain gages failed during the test. Failures that were easily identified include strain values that were either near zero or off-scale for the entire test. Partial failures that were slightly more difficult to identify are typically caused by construction equipment. These particular cases usually show strain gage data with standard deviations that are a large percentage of the mean during portions of the test. Each data set from each strain gage was evaluated on an individual basis to determine its validity. Figures A12, A13, and A14 show plots of typical data recorded during the dead load test.

Gage 612 in Figure A14 illustrates a gage deemed unreliable beyond approximately 12:00p.m. on Day 1.

The majority of the strain gages were concentrated around the girder connection. Strain diagrams have been produced displaying strain values from the gages with respect to their stage on each station. The strain values reported is the mean obtained by considering 60 samples taken consecutively over a specific 5 minute period. The y-axis represents the particular stage location on the girder, with the origin being the extreme fiber on the bottom of the steel girder. The x-axis represents the mean strain and is shown in microstrain, $\mu\varepsilon = 1\text{x}10^{-6}\ \frac{\text{in.}}{\text{in.}}$. Figures A15-A20 show the strain diagrams for six stations along girder 4 (station locations are identified in Table A2). Each figure contains four sets of strain gage data points that are each individually connected with a line. Each of the four data sets correspond to the time periods previously discussed in Section 5.1. For proper viewing of the strain diagrams, it is beneficial to use Figure A6 as a cross-reference. With only a few exceptions, girders 5 and 6 display strain behavior that is similar to girder 4. Figures A21 through A32 are strain diagrams for girders 5

and 6. Overall, the strain diagrams typically display behavior that is expected of girders with moment connections that provide continuity.

The centerline of the girder connection consists of a 2 x 18in. cover plate in tension coupled with a 2 x $23\frac{1}{2}$in. kicker wedge plate in compression. With reference to Figures A3 and A4, the developed areas of the compression and tension plates are approximately equal, and as a result, the compression and tension plates should exhibit approximately equal strains. Figures A15, A21, and A27 show that this did not occur during the dead load test. In fact, the kicker wedge plates display strain values that are approximately three times greater than expected. The strain gages were placed an approximate distance of 1in. clear from the edge of the weld joining the two kicker wedge plates. The kicker wedge plates were to be in direct bearing, but the large stresses may be the result of stress concentrations around the weld. This phenomena has been observed, but very little can be offered as an explanation. Several possibilities have been discussed among members of the research group, but the true behavior remains unknown. Some of the possibilities that were discussed are presented below.

- Bearing between the kicker wedge plates and girders is present, but the weld provides a stiffer path for load transfer between the kicker wedge plates.
- Bearing between the kicker wedge plates and girders was not achieved before the welds were placed, thus causing concentrated forces at the welds.
- Bearing was achieved between the kicker wedge plates and was subsequently lost overnight during thermal contraction of the girders. The welds were placed the following morning.

With reference to the strain diagrams in Figures A15, A21, and A27, there is a slight increase in the proportion of tensile strain in the cover plate to the compressive strain in the kicker wedge plate over the duration of the dead load test. This behavior is expected, and a more detailed discussion is provided in Section 5.5. A photograph of the kicker wedge plates at girder 6 is shown as Figure A33. This figure shows some of the difficulty associated with installing the wedge plates with only a minimal amount of clearance between the girders and the diaphragm reinforcing steel.

A small amount of deflection data was taken to supplement the large amount of strain data. A Pentax

Autolevel was used to measure the elevation of the bottom flange of all five girders during the different phases of the dead load test. The measurements were taken at a distance of 75ft. north of the south end of the girders. The top of a light pole foundation, located approximately 50ft. east of Massman Drive Bridge on the south side of I-40, was used as the elevation benchmark. Table A4 lists the absolute deflection of each girder during each phase of the dead load test. Figure A34 is a plot of the deflection data presented in Table A4 for girder 4.

5.3. Discussion of Data

This thesis involves the behavior of the experimental connection across the center bent as the girders are loaded with the dead load of the deck. The following discussion presents the observations that were extracted from the data.

The bridge deck was poured over a two day period. The first day's placement consisted of Phase 1 and 2, both positive moment regions. During data collection, there was some concern as to how much composite action would develop in the positive moment regions in one day. Figure A19 is a plot of the strain diagram in girder 4 near the region of maximum positive moment. With reference to this plot and

to corresponding Figures A25 and A31 for girders 5 and 6, it is evident that neither the neutral axis nor the strain diagrams underwent significant change during the different phases of the dead load test. For this reason, composite behavior was not believed to be significant in the analysis of this particular dead load test. The girder was calculated to have a strong axis moment of inertia approximately equal to $62{,}321 in^4$. At the connection centerline, the strong axis moment of inertia is approximately $73{,}389 in^4$.

The analysis of strains, stresses, and moments in prismatic beams is well documented. At the connection there is a steep stress gradient from the girders to the cover plate and kicker wedge plates. This complicated stress transfer precludes the use of typical analysis techniques, so a method in which sections were cut and free body diagrams drawn was used instead. The strains obtained during the test were converted to forces using the relation, $F = \varepsilon EA$. In this fundamental equation, F is the force in an element, ε is the measured strain, E is the modulus of elasticity, and A is the cross-sectional area of the element. Tests have shown that there is some difference between the actual strain in a specimen and the

measured strain from weldable strain gages. The tests show that E should be increased by 10% to account for this difference. In this thesis, E was taken as $32{,}000ksi$ when calculating stresses from strains measured by strain gages. After the forces had been determined, the internal bending moments were calculated using the following general procedure.

- At sections with at least two strain gages that displayed reliable strain plots, bending moments were calculated by summing moments about the theoretical centroid.
- At sections with one strain gage or only one reliable strain gage, bending moments were calculated by summing moments about the unknown or unreliable force. The Massman Drive Bridge is an indeterminate structure, so summing moments about a location other than the centroid may introduce some error when the axial force is not zero. Computer models of the structure show theoretical axial forces within each girder to be less than 1kip. However, measured values of axial force were found to be substantially more than what theory suggests.

The methods outlined above appeared to be very reliable and were programmable using conventional computer software. As always, stations with only one strain gage sometimes displayed questionable results. In particular, station 2 of girder 5 had a measured moment inconsistent with adjacent gages. Since there was only one strain gage at this station, the data point was eliminated.

The strain gages were balanced with the reinforcing steel, construction equipment, and formwork in place, so the unit weight of concrete was taken as $145\frac{\text{lb.}}{\text{ft}^3}$. The 368yd^3 of total concrete placed for the bridge deck resulted in tributary loads of $1.064\frac{\text{kip}}{\text{ft.}}$ for interior girders and $0.914\frac{\text{kip}}{\text{ft.}}$ for exterior girders. For calculation ease, the static moment is computed with the relation $M_{static} = \frac{wl^2}{8}$ even though the 3.5ft. length of bridge deck of phase 5 had not been placed at Time 3. In the equation, M_{static} is the difference between the moment at midspan and the average of the moment at the supports, w is the load per unit length, and l is the span length. The calculated static moment is 2,816kip-ft. and 2,419kip-ft. for interior and exterior girders, respectively.

The calculated static moments were used as a normalization tool for the measured static moments at Time 3. The calculated and measured static moments for girder 4 were determined to have a percent difference of 11%. Girders 5 and 6 were found to have a percent difference between their calculated and measured static moments of 40% and 44%, respectively. The measured static moment is very sensitive to the moment value at the midspan of the girder. Unfortunately, this is one of the few locations along the girders where there are very limited data. As a result, it was decided to use the flexure formula to calculate moments at stations 6 and 7 of girder 5 and station 7 of girder 6. In the flexure formula, $\sigma = -\frac{My}{I}$, σ is the flexural stress, M is the bending moment, y is the distance from the neutral axis, and I is the moment of inertia. Substituting the relation between stress and strain, $\sigma = \varepsilon E$, into the flexure formula and solving for M yields $M = -\frac{\varepsilon E I}{y}$. After the normalization procedure, girders 5 and 6 were found to have a percent difference between their calculated and measured static moments of 31% and 24%, respectively.

The measured internal moments for Time 3 are presented in Figures A35, A36, and A37 as moment diagrams for girders

4, 5, and 6, respectively. The origin of the x-axis represents the centerline of the connection at the center bent, and the y-axis is the measured moment. The data points have been fit with a second-order polynomial that is shown as a solid black line. Figure A6 may be helpful as a cross-reference while viewing the moment diagrams.

From Figures A35, A36, and A37, it is apparent that girder 6 behaves differently from girders 4 and 5 in terms of measured maximum negative moment. With reference to Table A4, girder 6 displays deflections throughout the loading period that are closer to those of interior girders than to the other exterior girder, girder 2. While a plot of the measured negative moments and total deflections for each of the time periods would be useful, a problem exists since deflection data were only measured near mid-span on the south side of the center bent. Based on the Visual Analysis model described in Section 5.4, deflections were calculated for locations 70ft. north of the connection centerline. The summation of the calculated and measured deflections at the two locations is useful when compared to the measured negative moments. With the deflections plotted on the x-axis and the negative moments plotted on the y-axis, the slope of the line that best fits the data

is a measure of connection stiffness. The plot of the measured maximum negative moment versus total deflection for each girder is presented as Figure A38. It is understood that combining measured and calculated data introduces error; however, the same error bias is applied to each girder in equal proportion. With this type of plot, a qualitative comparison can be made between the moment-deflection behavior of the connection of girders 4, 5, and 6, and that is the only intent. Each of the three data sets have been fit with a first-order regression line. In Figure A38, the regression lines for girders 4 and 5 show that they have similar stiffness values.

5.4. Computer Model

The theoretical behavior of the bridge girders was modeled using Visual Analysis 4.0, developed by Integrated Engineering Software, Inc. (IES, Inc.). Visual Analysis is a finite element structural analysis program that lends itself to low complexity models of materials in the elastic range with small rotations and deflections.

With the girder dimensions, loading information, and support conditions outlined above, Visual Analysis produced the moment diagrams in Figures A39 and A40 for the interior and exterior girders, respectively. The dashed black line

is the theoretical moment diagram. Combined plots of measured and theoretical moment diagrams for each time period for each of the girders are shown as Figures A41 through A52.

5.5. Discussion of Results

The strain diagrams shown in Figures A15-A32 and discussed in Section 5.2 all show behavior of girders and moment connections with continuity across the center bent. For all three girders, the moment diagrams in Figures A41-A52 show that moment is transferred through the connection to the adjacent girder throughout the dead load test. Therefore, the strain and measured moment diagrams presented in this thesis indicate continuity was achieved across the experimental connection at the center bent.

Based on Figures A35, A36, and A37, it is evident that the maximum negative moment for girders 4 and 5 are comparable. Girders 4 and 5 have maximum negative moment values of -2,300kip-ft. and -2,100kip-ft., respectively. These two moment values vary from the theoretical moment values, discussed in Section 5.4, by 18% and 23%, respectively. Conversely, girder 6 exhibits a maximum negative moment of -1,100k-ft, which varies from its theoretical equivalent by 53%. From the moment diagrams

and the moment deflection plot in Figure A38, it can be deduced that girder 6 is not as stiff as girders 4 and 5. Since the three girders are identical, except for girder 6 having five fewer web stiffeners, it can be concluded that the connections at girder 4 and 5 are stiffer than the connection at girder 6.

It is not entirely known why there is a reduced stiffness in the connection at girder 6. The rationale proposed by the author involves the kicker wedge plates and their installation in the structural system. Figure A53 is a photograph of the connection at girder 6 showing the kicker wedge plates before they are driven to bear against the bottom flanges of the two girders. Review of the photograph shows a distinct difference between the area of potential contact between the bottom flange of the girder and the kicker wedge plate for the joint on the left and on the right. This apparent reduced compressive area as a result of the plate end geometry will cause a reduced moment of inertia and connection stiffness.

The computer model discussed in Section 5.4 was used to determine the effect of the reduced compressive area at the connection. In the model, the depth of bearing was incrementally reduced from the design thickness of 2in. to

0.40in. As the compressive area is reduced, the connection moment of inertia is reduced and the centroid of the connection moves closer to the cover plate. At the thickness limit of 0.40in., the connection moment of inertia is 28,500in^4. Using these modified quantities, the computer model shows maximum compressive stresses in the connection to be near the yield stress of 50ksi. The Visual Analysis computer model only operates in the elastic range and cannot be used further. More detailed analysis techniques are possible with other finite element software, but detailed plastic analysis techniques could require detailed three-dimensional profiles of the surfaces in bearing.

5.6. Conclusions

Conventional highway bridges across the state of Tennessee generally fall under two main categories. These include simple span or continuous bridges constructed of steel or reinforced concrete girders. During construction, simple span steel girders need only be placed on the foundation supports; continuous girders require bolting and/or welding of field splices to complete the connections. On two span bridges, there are typically three girder segments that require two field splices. Once

constructed, continuous span bridges have advantages over simple span bridges since they are able to distribute moments to every span; while, simple span bridges must resist the loads in the particular span of load application.

The Massman Drive Bridge is an experimental design that unifies the construction economy of simple span bridges and the structural economy of continuous span bridges. The bridge girders are initially erected having simple supports. The experimental connection, consisting of cover plates and kicker wedge plates, is then used to connect the two adjoining girders over the center bent. As a result, the bridge is designed to function as a continuous bridge during the deck pour. During construction of the parapets and service under traffic, the bridge is designed to be continuous across the center bent with the steel girders behaving compositely with the reinforced concrete deck.

Several conclusions can be drawn from the data presented. It has been shown that continuity was achieved in girders 4, 5, and 6 during application of the dead load of the deck. However, it has also been shown that the connection stiffness varied between that in girders 4 and 5

and that in girder 6. A rationale was presented in Section 5.5 to attempt to explain the cause of the reduced stiffness, but the rationale is difficult to either confirm or deny.

Considerable attention is given to moment connections in the design of steel structures. There have been many research projects devoted to topics related to conventional bolted connections. For instance, weld strength, bolt strength, friction between steel that is both painted and unpainted, and steel fatigue are heavily documented along with ample amounts of specifications for quality control. Even with that, bolted moment connections in highway bridges are typically only placed near moment inflection points (i.e. locations of minimal moment). On the Massman Drive Bridge, the moment connection is located at the point of absolute maximum moment. There are 144, 1in. diameter, A490 Grade 50W bolts that are torqued to AASHTO specifications to achieve a slip critical connection in the tensile cover plate. In contrast, the kicker wedge plate installation undergoes very little quality control even though good bearing conditions are required for the connection to perform as designed. It is recommended that a more thorough quality inspection program be implemented

to ensure that the desired connection is built accordingly. The level of inspection should be commensurate with the degree of criticality of its proper operation.

The principle conclusion drawn from the research on the Massman Drive Bridge is that continuity over the center bent under the dead load of the fluid bridge deck concrete was provided. Even though the connection at girder 6 showed a reduced stiffness, the overall conclusion is that the method works; the bridge may reasonably be designed as a continuous bridge under the weight of the concrete deck.

6. CONTINUED RESEARCH

6.1. Other Dead and Live Load Tests

During the Spring of 2005, several controlled load tests were performed on the Massman Drive Bridge. These tests include the following.

- A fully loaded dump truck (75kip) was used to test the bridge under live load before the parapets were constructed.
- A dead load test was conducted to determine the behavior of the continuous and composite bridge under the dead load of the parapets.
- A fully loaded dump truck (75kip) was again used to test the bridge under live load. During this test the parapets had been placed and cured, so their contribution can be considered in the analysis.

The data from these tests are of good quality and will likely produce useful results. Pending approval of a research proposal, further data analysis will be done.

The Massman Drive Bridge is currently open to traffic. A photograph of the completed bridge is shown as Figure A55.

References and Bibliography

References and Bibliography

American Association of State Highway and Transportation Officials (AASHTO) (1998). *AASHTO LRFD Bridge Design Specifications*, 2nd Edition, Washington, D.C.

Azizinamini, Arnold, Lyndon Vander Veen (November 2004), *Bridges Made Easy*, Roads & Bridges Volume:42 Number:11.

Bryant, Boudleaux, Felice Bryant (1967), *Rocky Top*, House of Bryant Publications.

Burdette, Edwin, J. Harold Deatherage, David W. Goodpasture, Earl Ingram (September 2004), *Final Report, Evaluation of Experimental Bridge: Dupont Access Bridge in Humphreys County*.

Chapman, David P. (May 2005), *Evaluation Of The Dupont Access Bridge*, Thesis presented to the University of Tennessee, Knoxville, TN, in partial fulfillment of the requirements for the Master of Science degree.

Gere, James M., Stephen P. Timoshenko, (1997), Mechanics of Materials 4th Edition, PWS Publishing Company, Boston, MA.

Hibbeler, Russell C., (1999), Structural Analysis 4th Edition, Prentice-Hall, Inc., Upper Saddle River, NJ.

Kulak, Geoffrey L., John W. Fisher, John H. A. Struik (2001), Guide to Design Criteria for Bolted and Riveted Joints, Research Council on Structural Connections.

Appendix:

Tables and Figures

Table A1: Girder and Gage Descriptors

Girder	Gage
4	4XX
5	5XX
6	6XX

Table A2: Station and Gage Descriptors

Station	Gage	Distance from Connection Centerline
1	X1X	0.0ft.
2	X2X	1.0ft.
3	X3X	1.5ft.
4	X4X	3.0ft.
5	X5X	4.3ft.
6	X6X	5.5ft.
7	X7X	76.0ft.
8	X8X	142.5ft.

Notes: Gage cross-section distances are measured from the connection centerline at the center bent.

Table A3: Stage and Gage Descriptors

Stage	Gage	Distance from Girder Bottom	Notes
1	XX1	65.5in.	Cover plate
2	XX2	65.5in.	Cover plate
3	XX3	61.5 or 62.0in.	Bottom of top flange
4	XX4	41.5 or 42.0in.	Top portion of web
5	XX5	21.5 or 22.0in.	Bottom portion of web
6	XX6	1.5 or 2.0in.	Top of kicker wedge plate or top of bottom flange
7	XX7	1.5 or 2.0in.	Top of kicker wedge plate

Notes: Since the bottom flange thickness is effectively either 1.5 or 2in. thick, the distance values for each of the stages are dependent upon the particular station of the strain gage.

Table A4: Girder Deflections at 75ft. north of South Abutment

	Girder				
	2	**3**	**4**	**5**	**6**
	Deflection (in.)				
Time 0	0.00	0.00	0.00	0.00	0.00
Time 1.5	-2.28	-2.46	-2.40	-2.34	-2.40
Time 2	-1.74	-1.92	-1.92	-1.80	-1.86
Time 3	-2.22	-2.34	-2.34	-2.16	-2.34

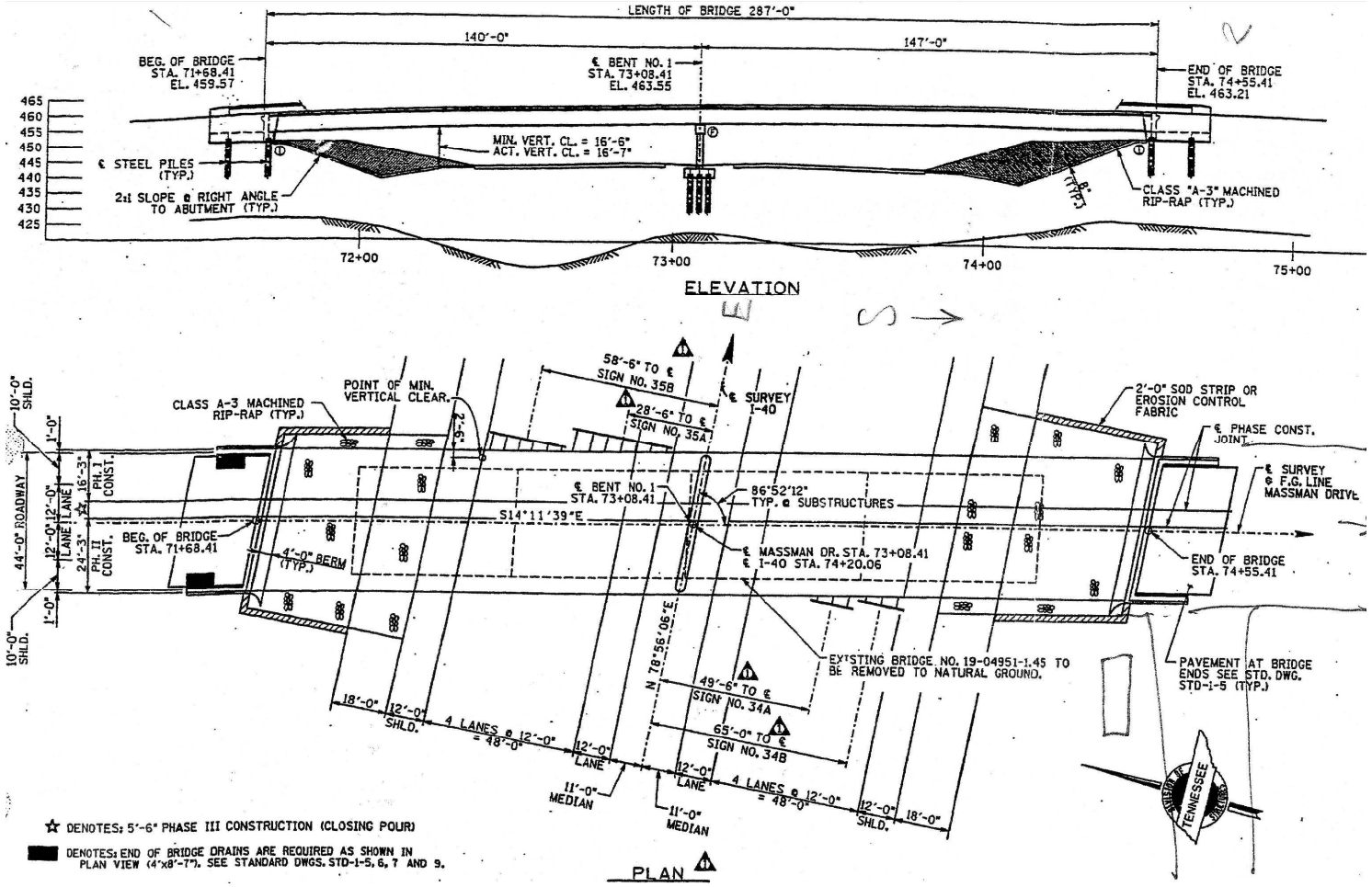

Figure A1: Elevation and Plan Drawing of Massman Drive Bridge

(Reproduced from TDOT's design plans)

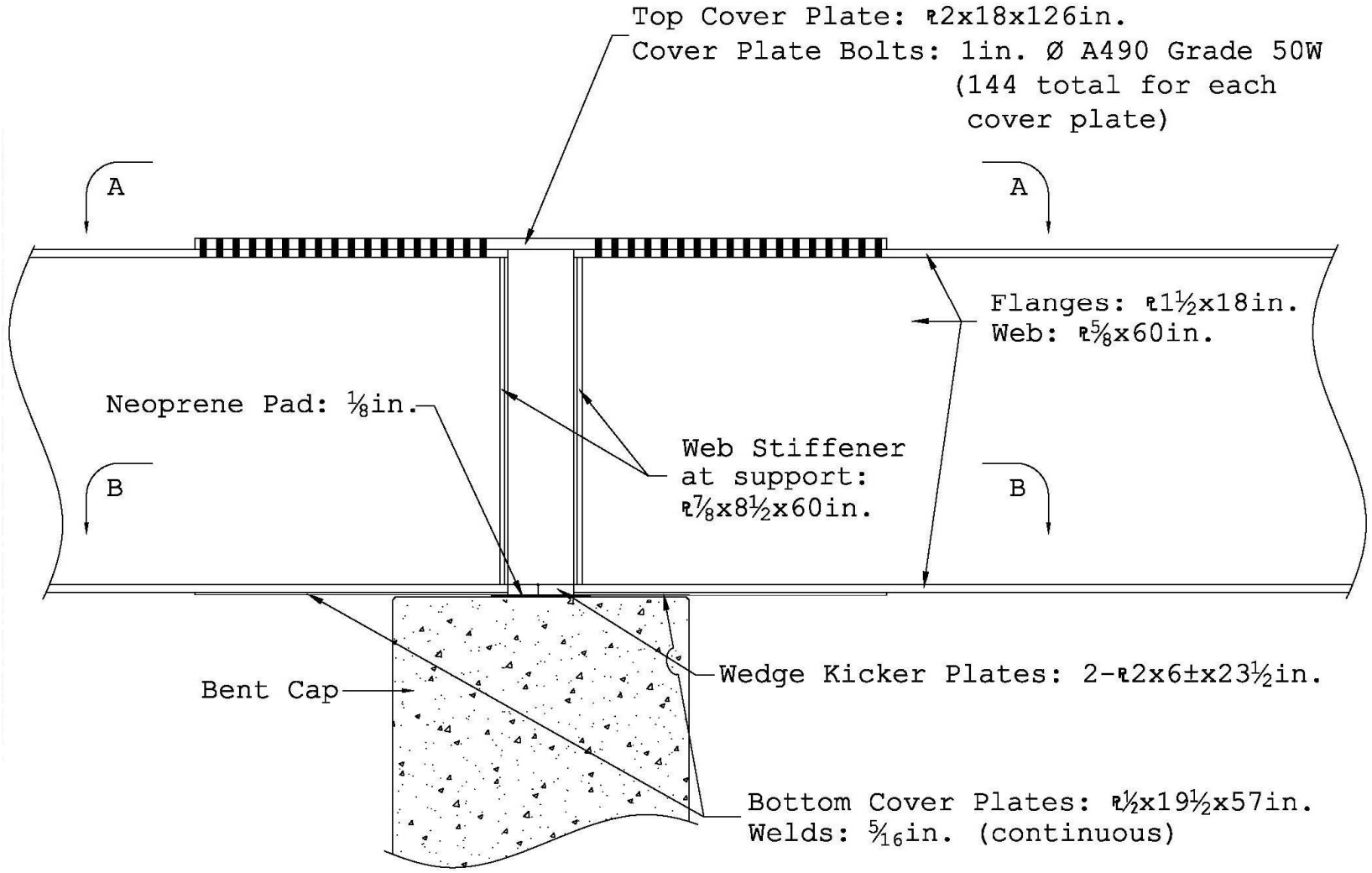

Figure A2: Elevation Schematic of Connection at Center Bent

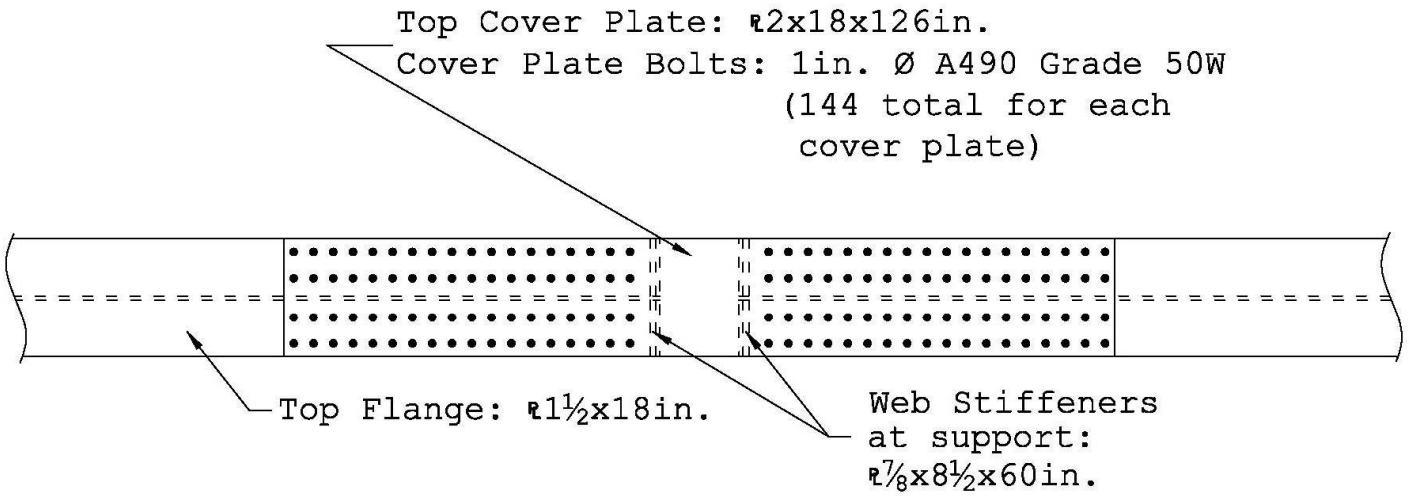

Section A - A

Figure A3: Plan Schematic of Top Cover Plate of Connection

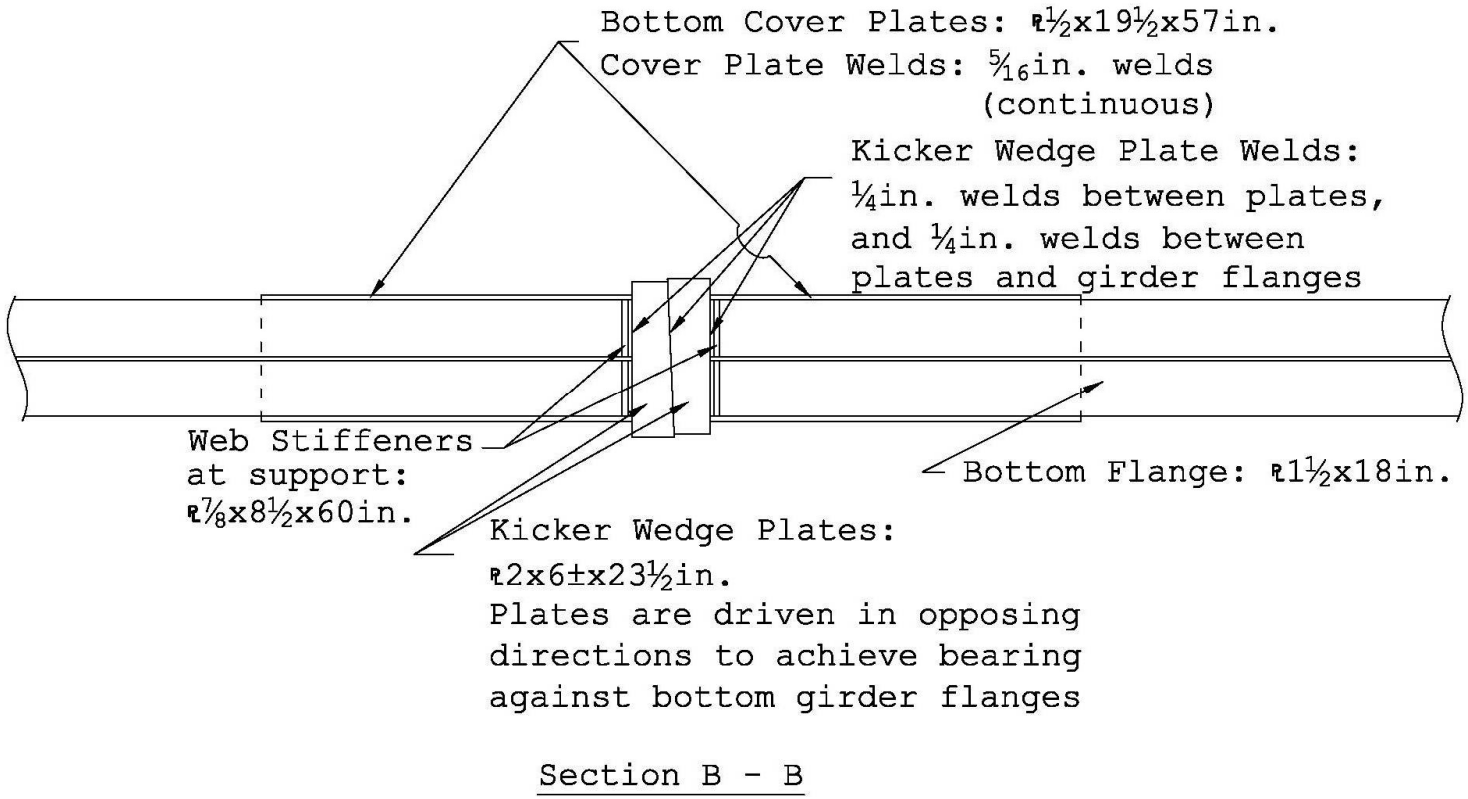

Figure A4: Plan Schematic of Bottom Cover Plates/Kicker Wedge Plates of Connection

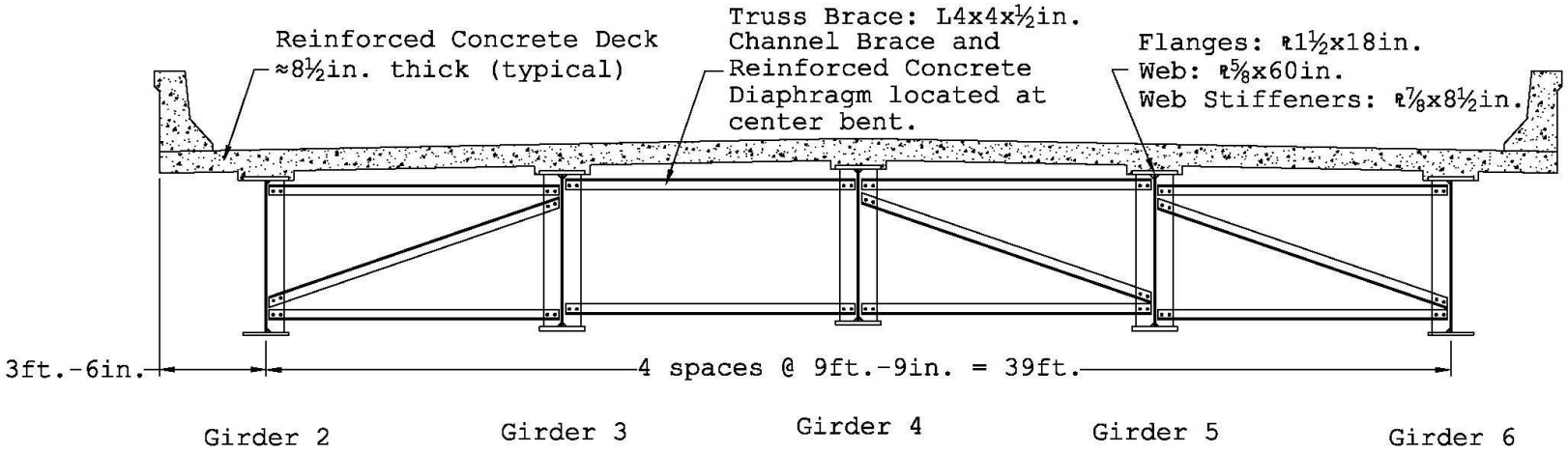

Notes:
-All structural steel is A709 Grade 50W, unless noted otherwise.
-Bolts are typically A325 Type 3. However, bolts at the center bent connection are A490 Grade 50W.
-All reinforcing steel is A615 Grade 60, unless otherwise noted.
-Bridge deck concrete is TDOT Class "D" (f'_c=4000 psi)

Figure A5: Cross Section of Massman Drive Bridge
(Section is taken with a view to the south)

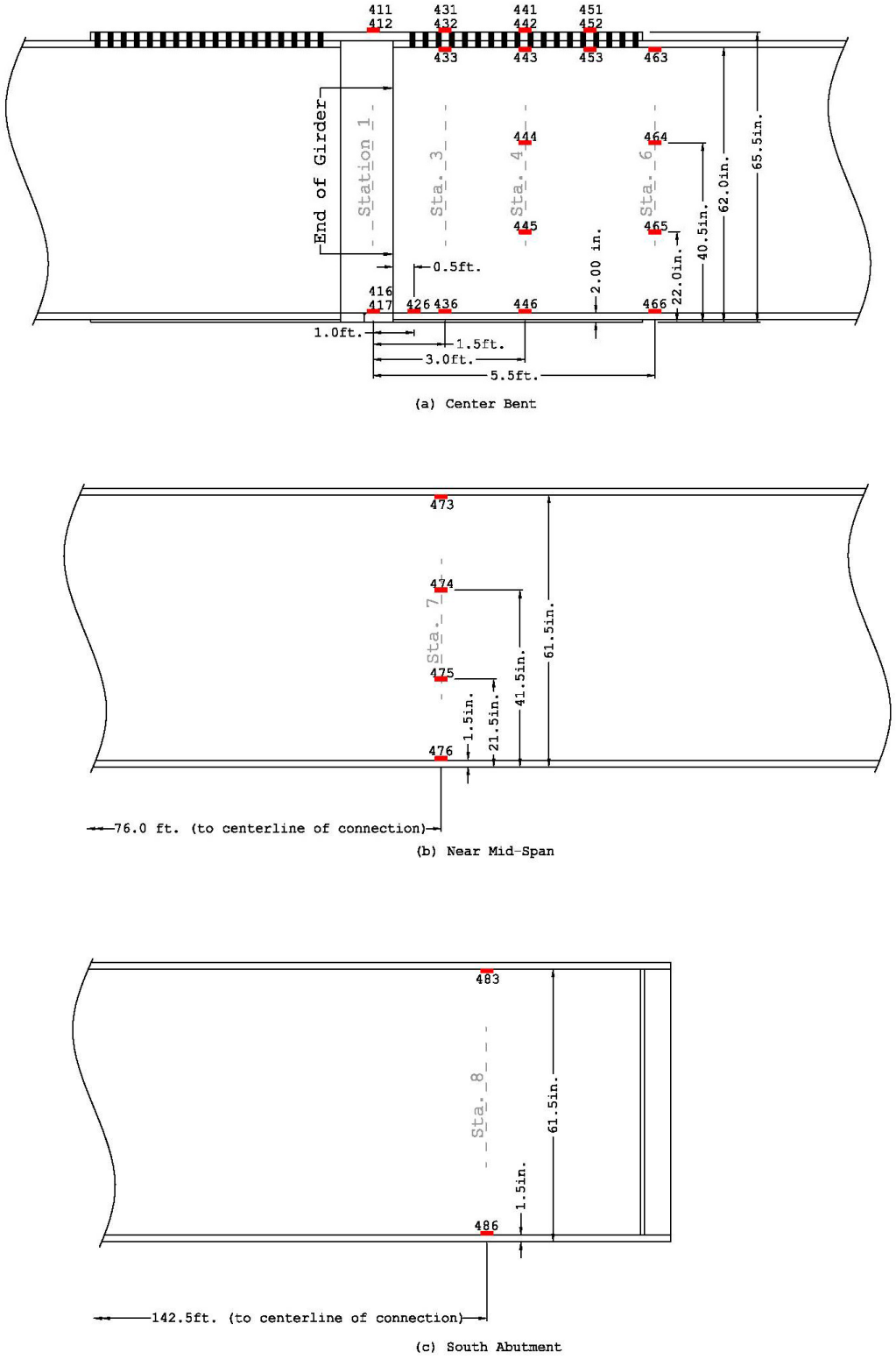

Figure A6: Girder 4 Elevation with Strain Gage Locations

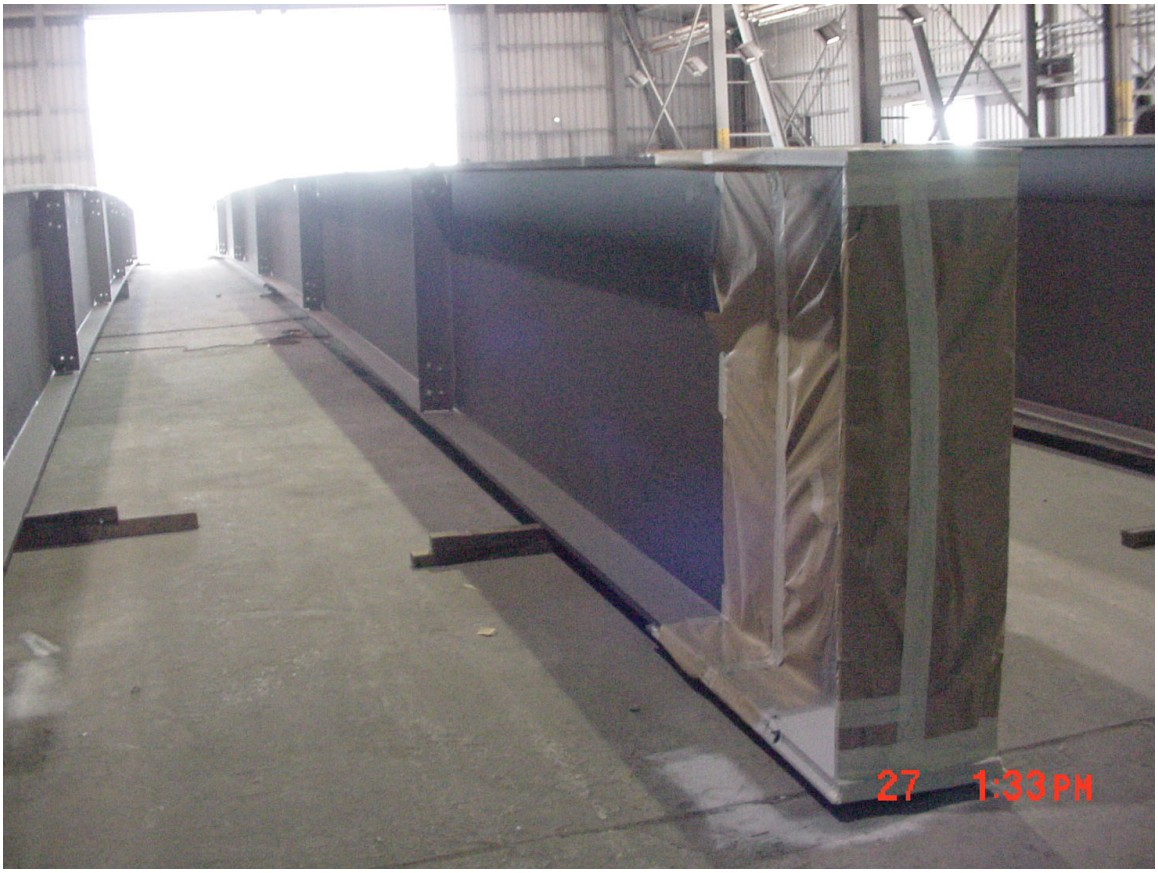

Figure A7: Photograph of Bridge Girders at the Fabricator

Figure A8: Phototograph of Strain Gages and Wires After Installation

Figure A9: Photograph of Girders After Being Erected

(View from the South Abutment)

Figure A10: Photograph of Connection Before Bolt Installation (View looking west at Girder 6 from Girder 5)

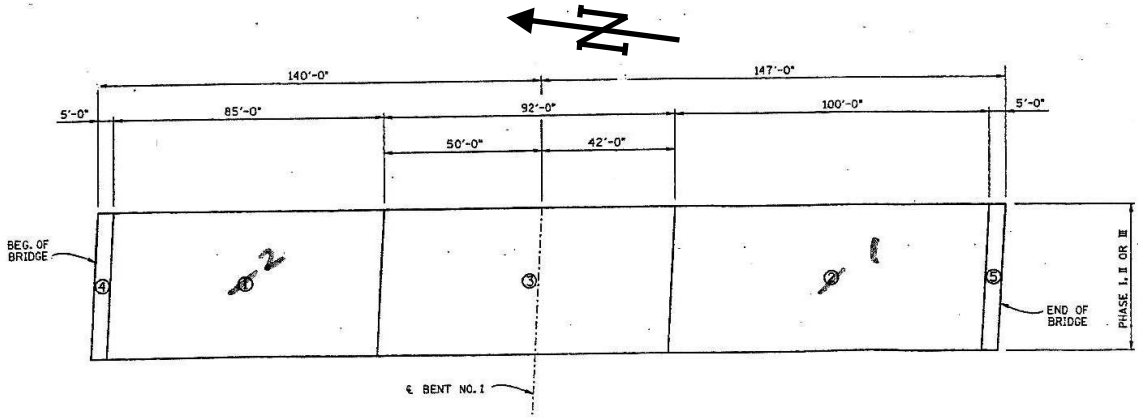

Figure A11: Deck Concrete Pouring Sequence Sketch

(Reproduced from TDOT's design plans)

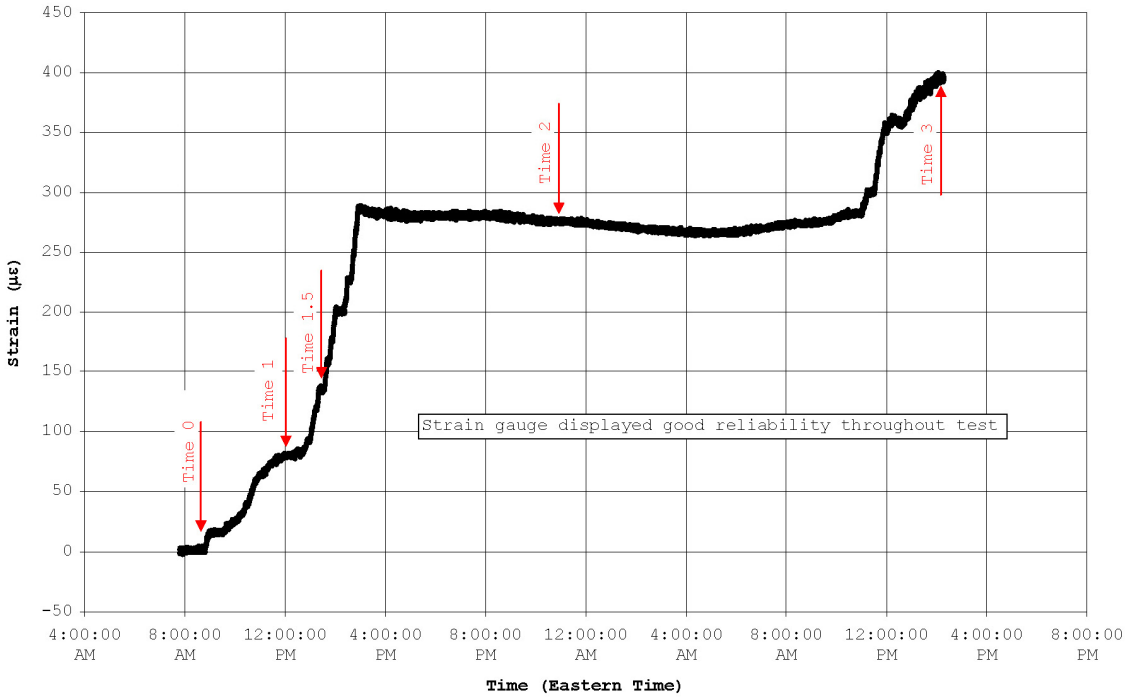

Figure A12: Data Plot for Strain Gage 411

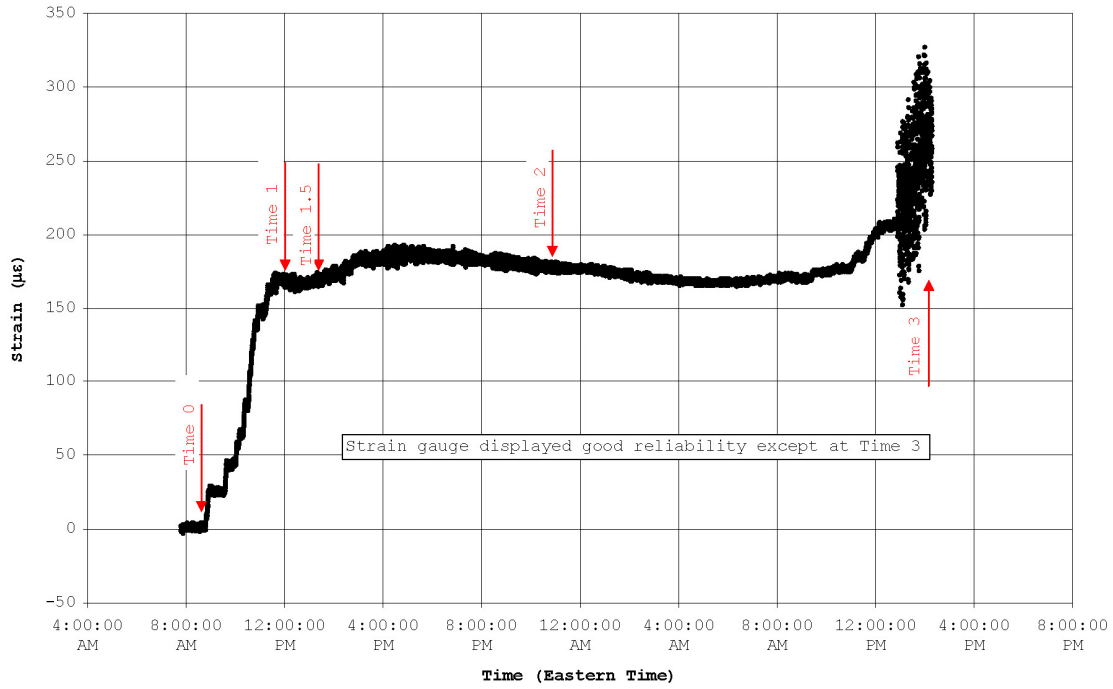

Figure A13: Data Plot for Strain Gage 532

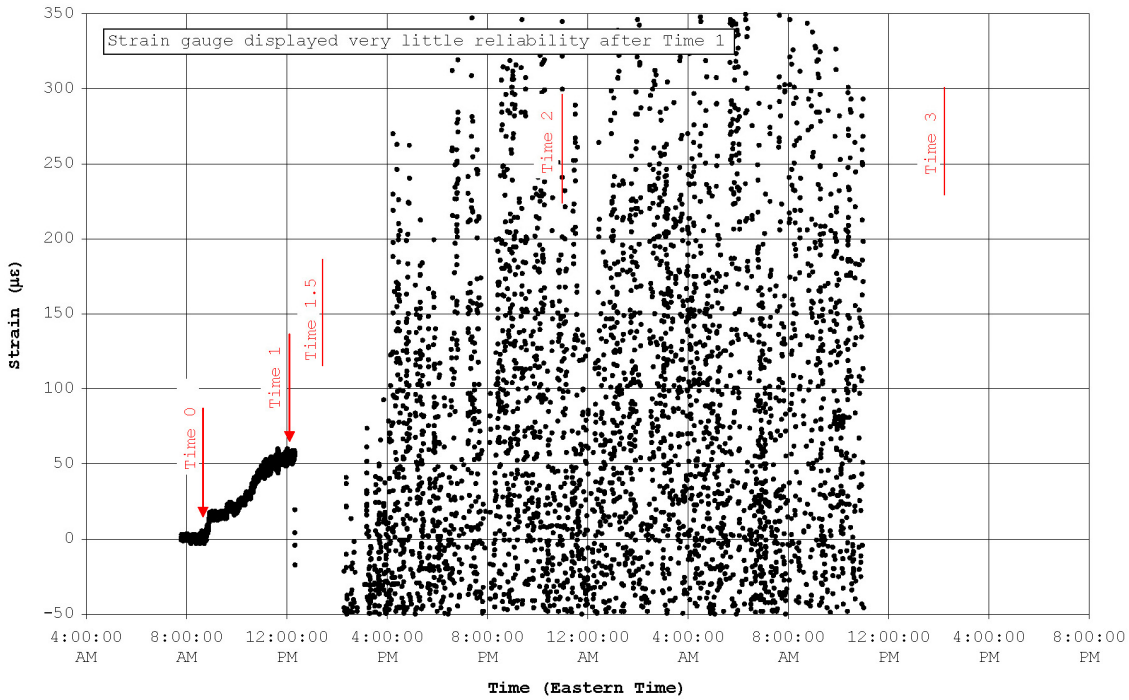

Figure A14: Data Plot for Strain Gage 612

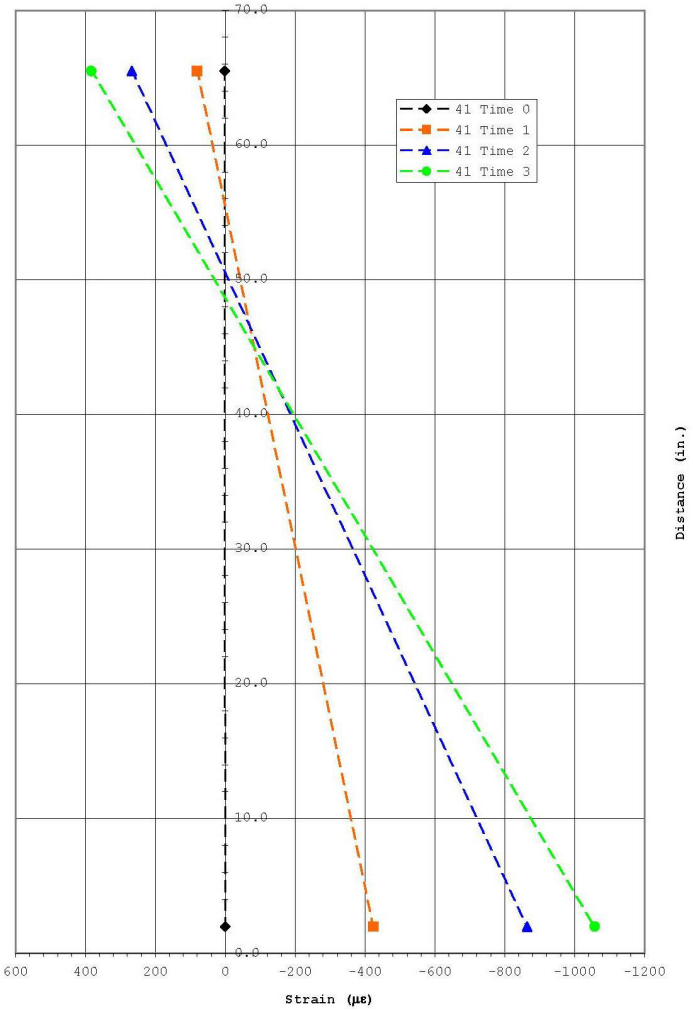

Figure A15: Strain Diagram of Station 1 on Girder 4

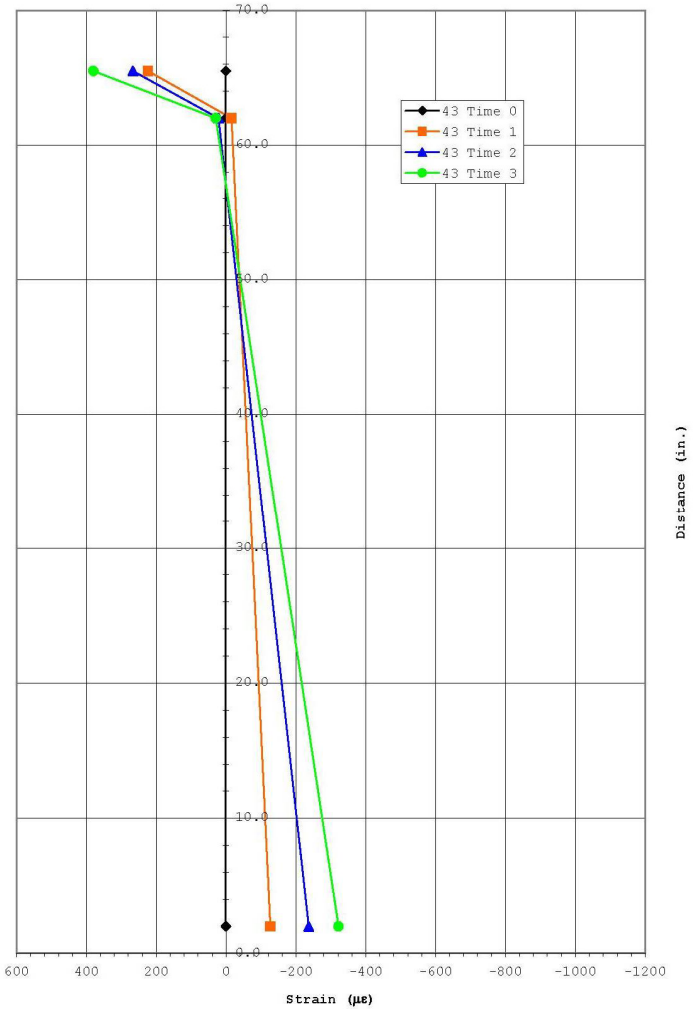

Figure A16: Strain Diagram of Station 3 on Girder 4

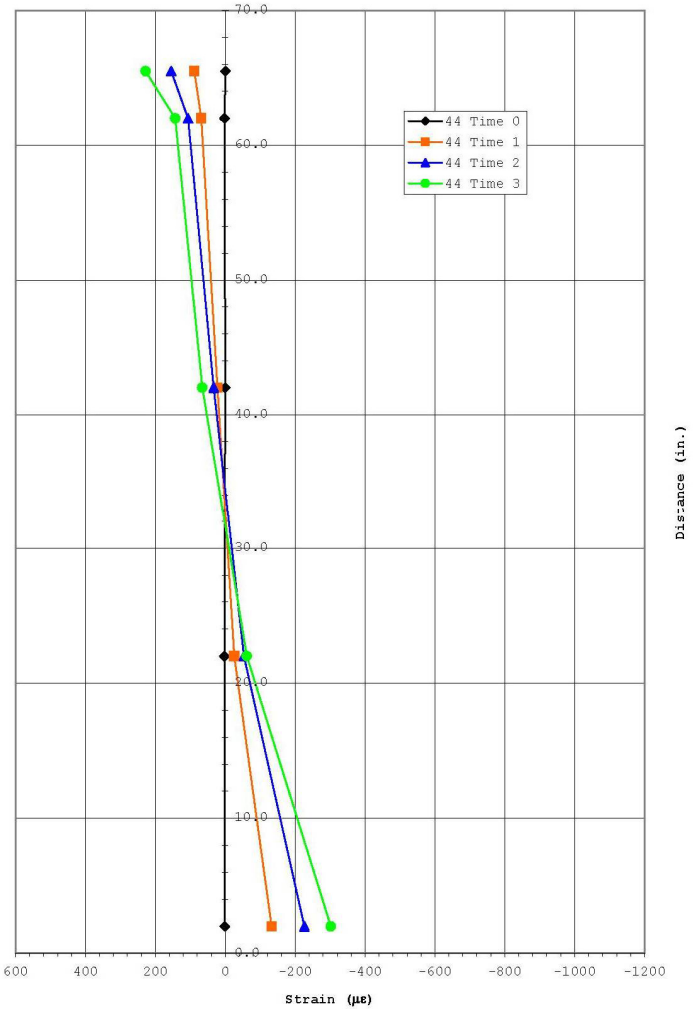

Figure A17: Strain Diagram of Station 4 on Girder 4

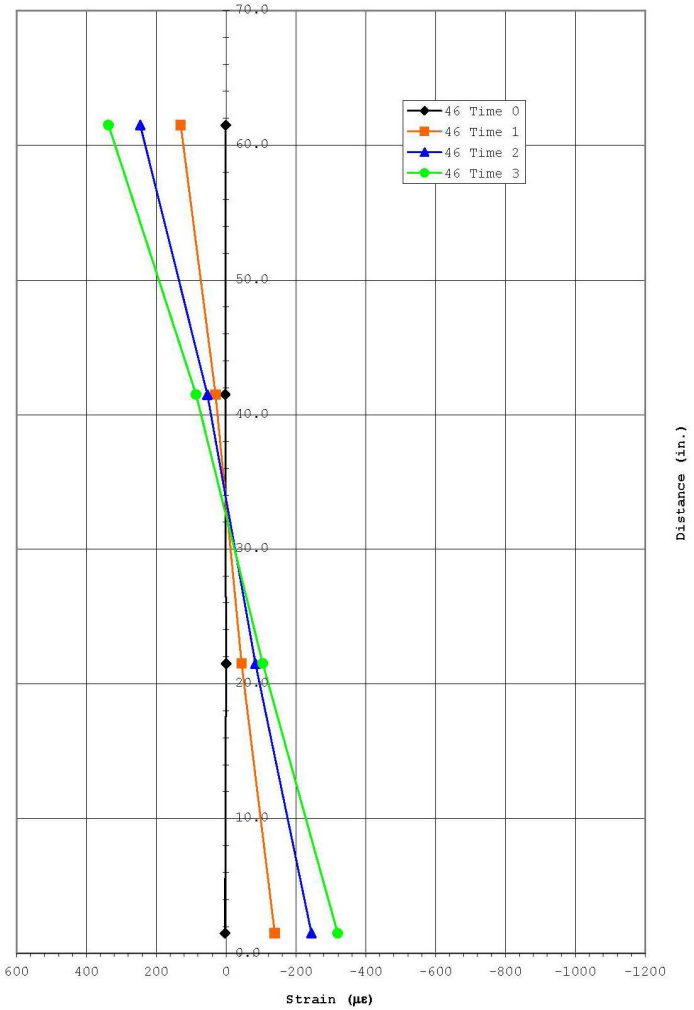

Figure A18: Strain Diagram of Station 6 on Girder 4

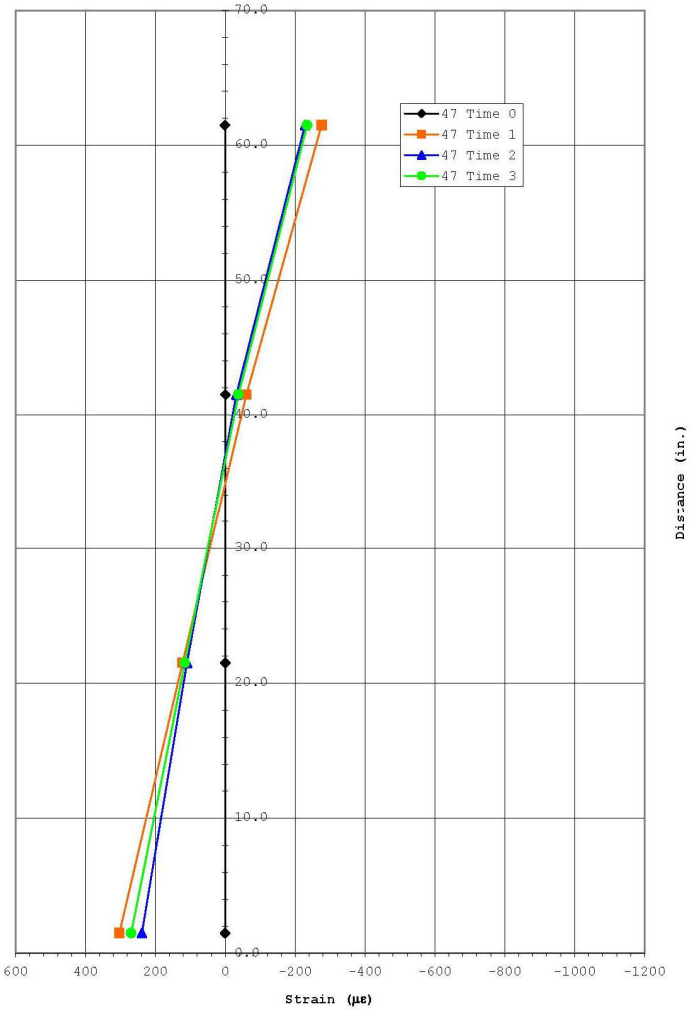

Figure A19: Strain Diagram of Station 7 on Girder 4

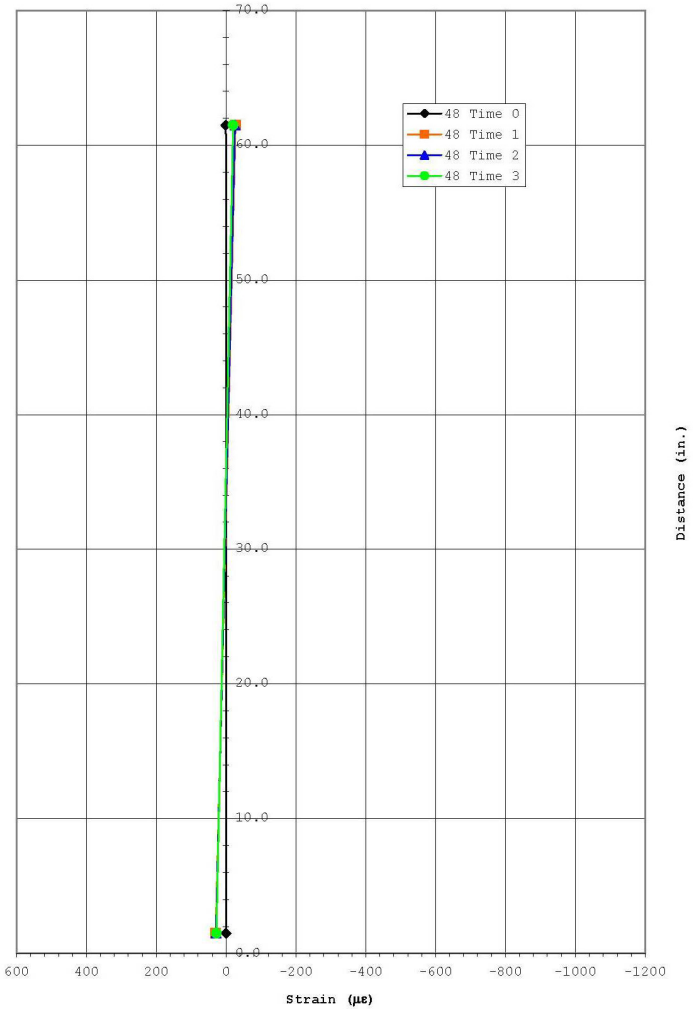

Figure A20: Strain Diagram of Station 8 on Girder 4

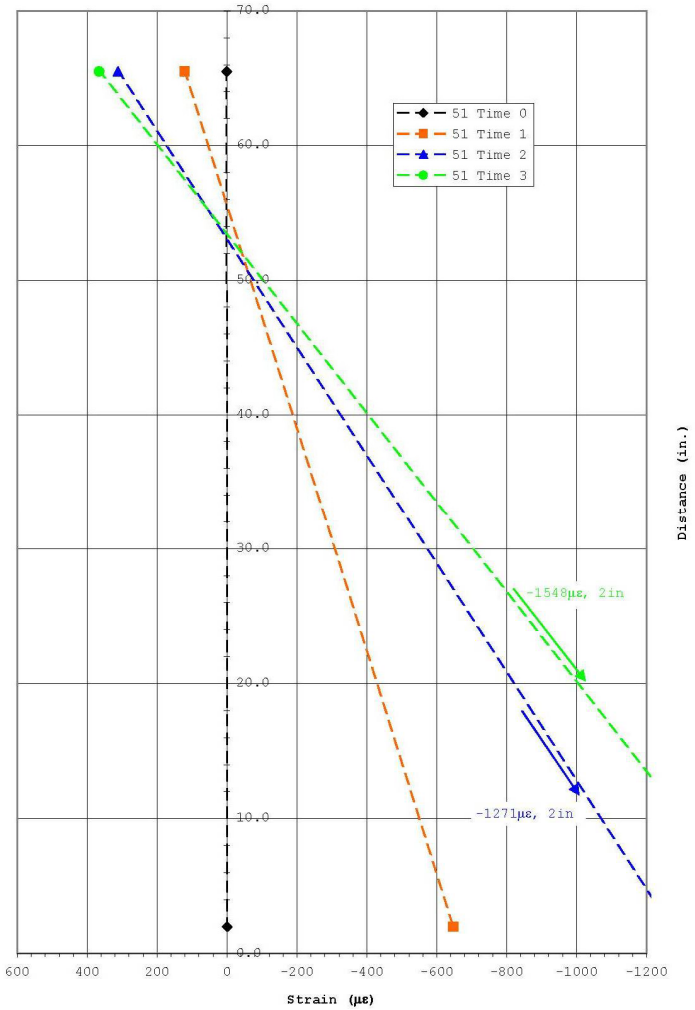

Figure A21: Strain Diagram of Station 1 on Girder 5

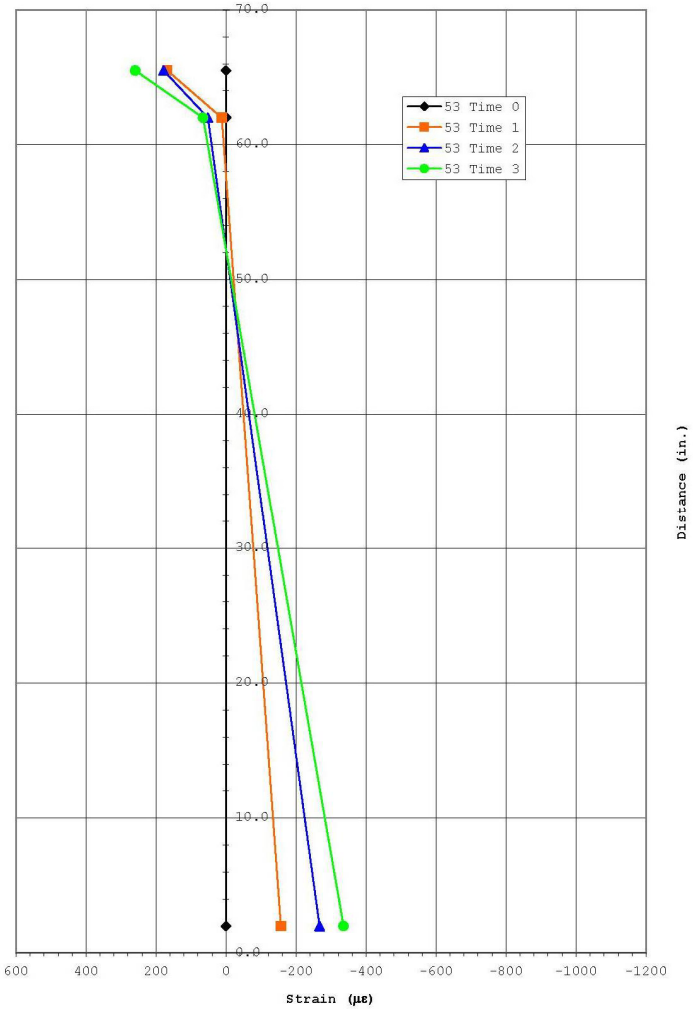

Figure A22: Strain Diagram of Station 3 on Girder 5

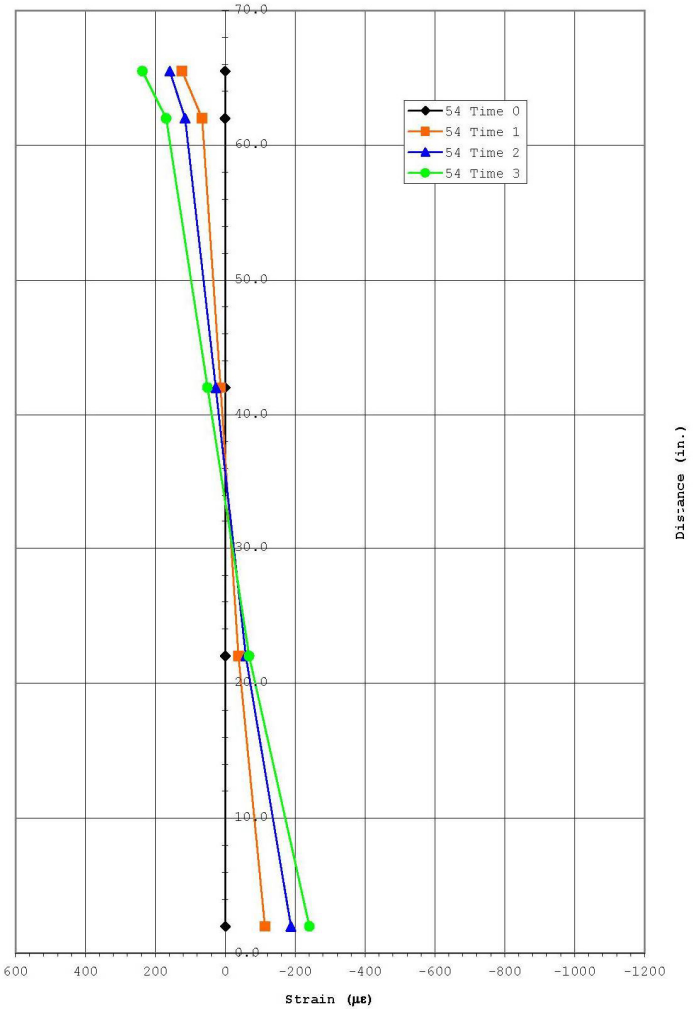

Figure A23: Strain Diagram of Station 4 on Girder 5

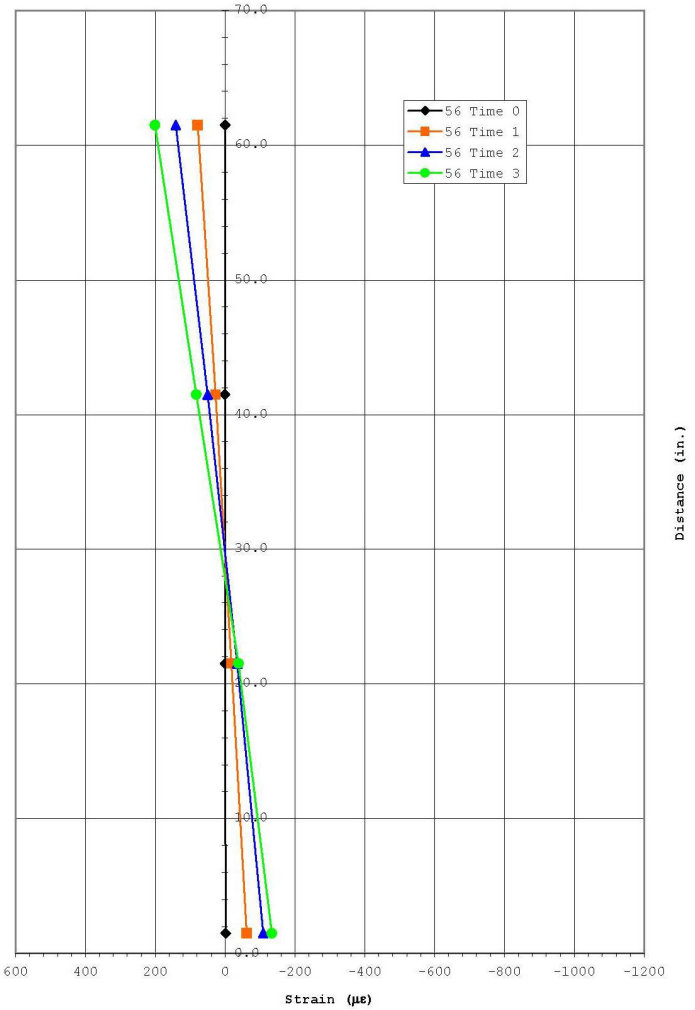

Figure A24: Strain Diagram of Station 6 on Girder 5

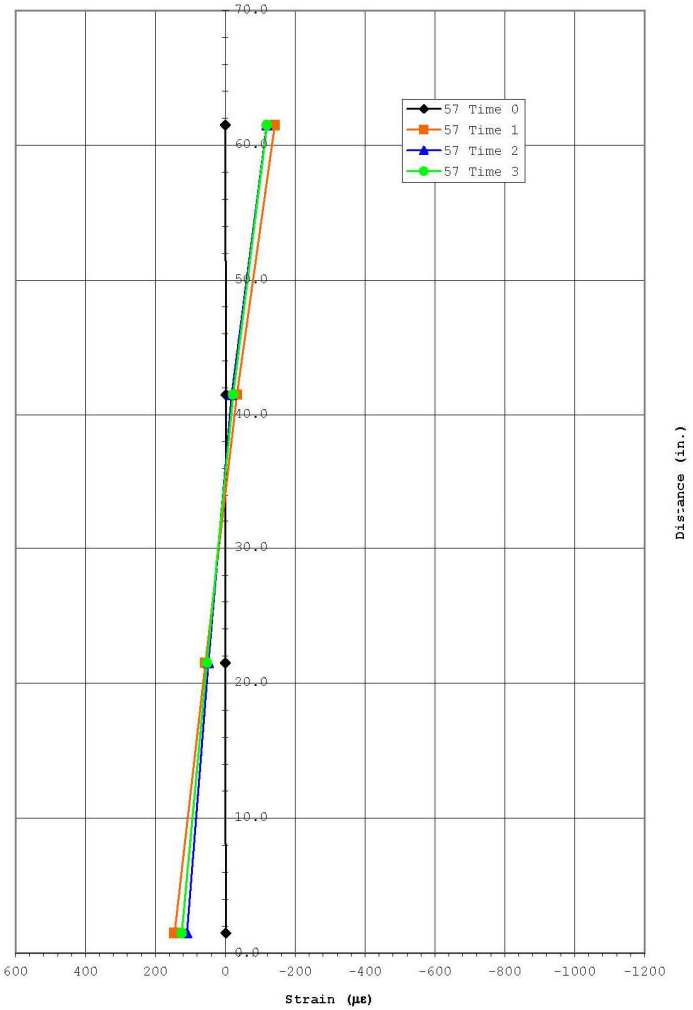

Figure A25: Strain Diagram of Station 7 on Girder 5

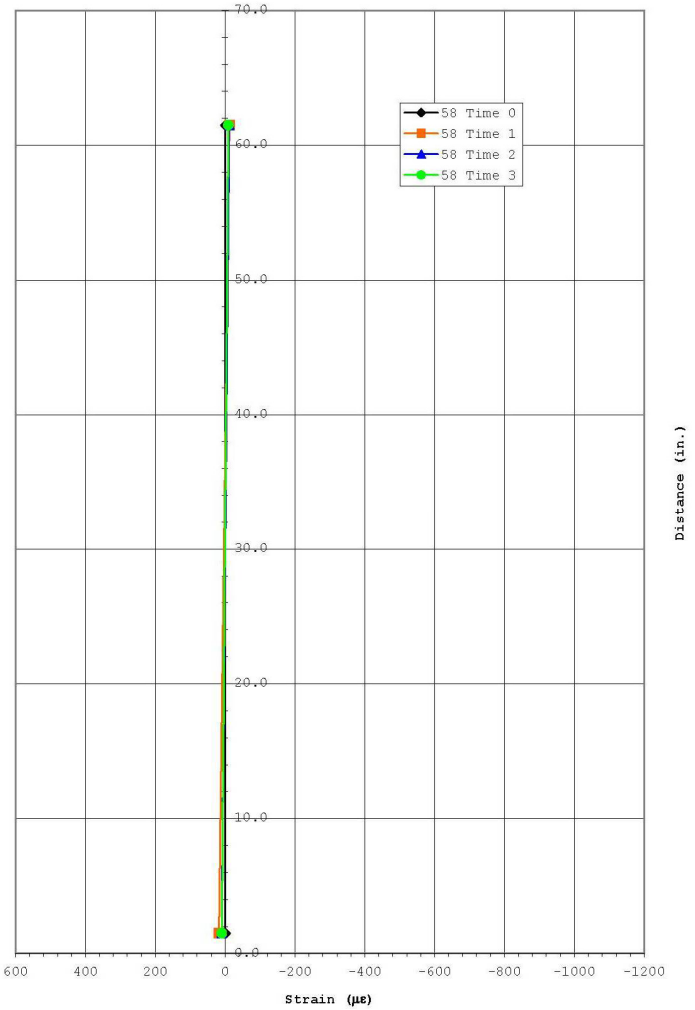

Figure A26: Strain Diagram of Station 8 on Girder 5

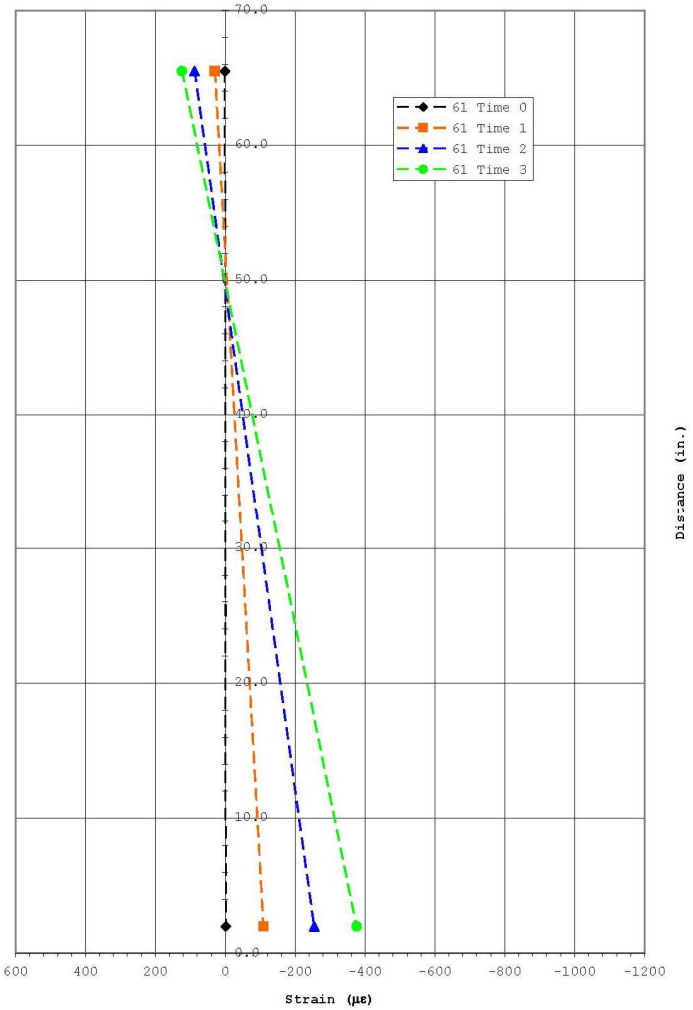

Figure A27: Strain Diagram of Station 1 on Girder 6

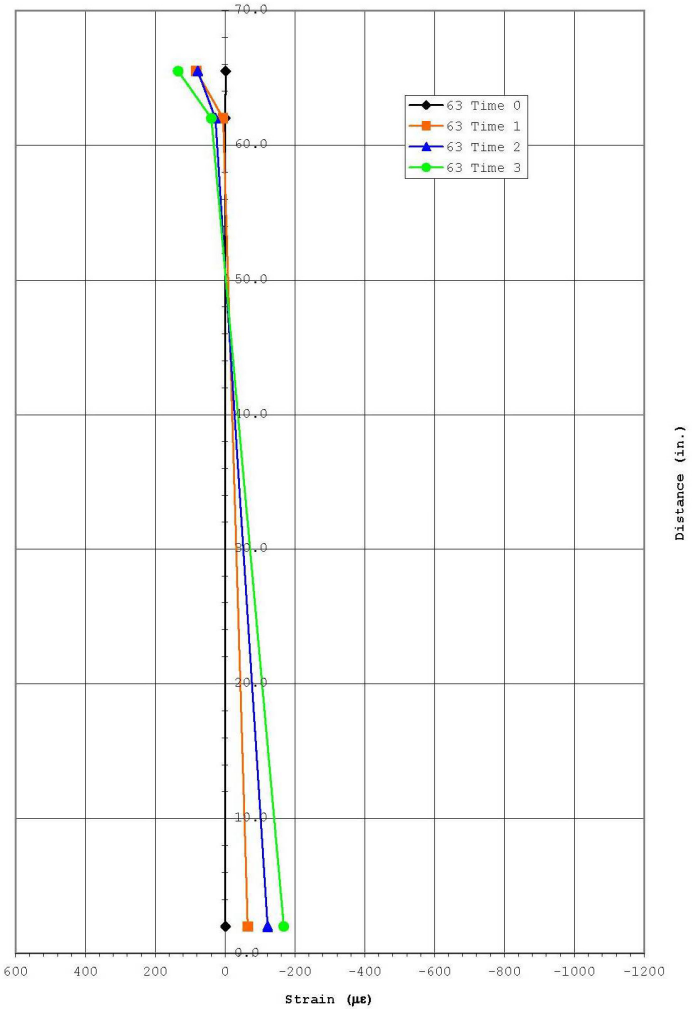

Figure A28: Strain Diagram of Station 3 on Girder 6

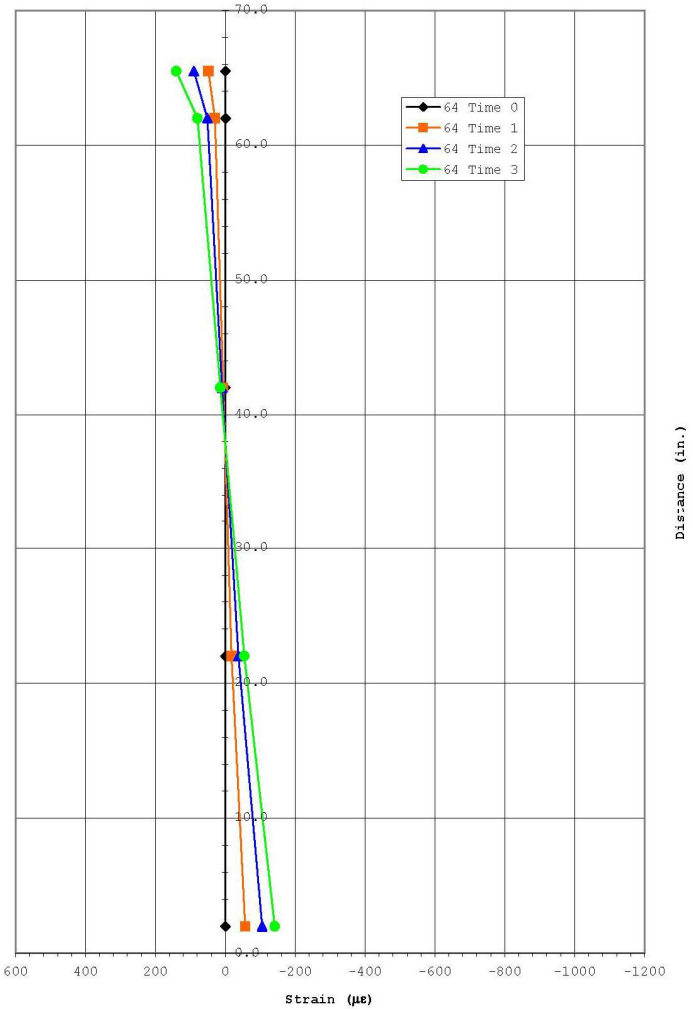

Figure A29: Strain Diagram of Station 4 on Girder 6

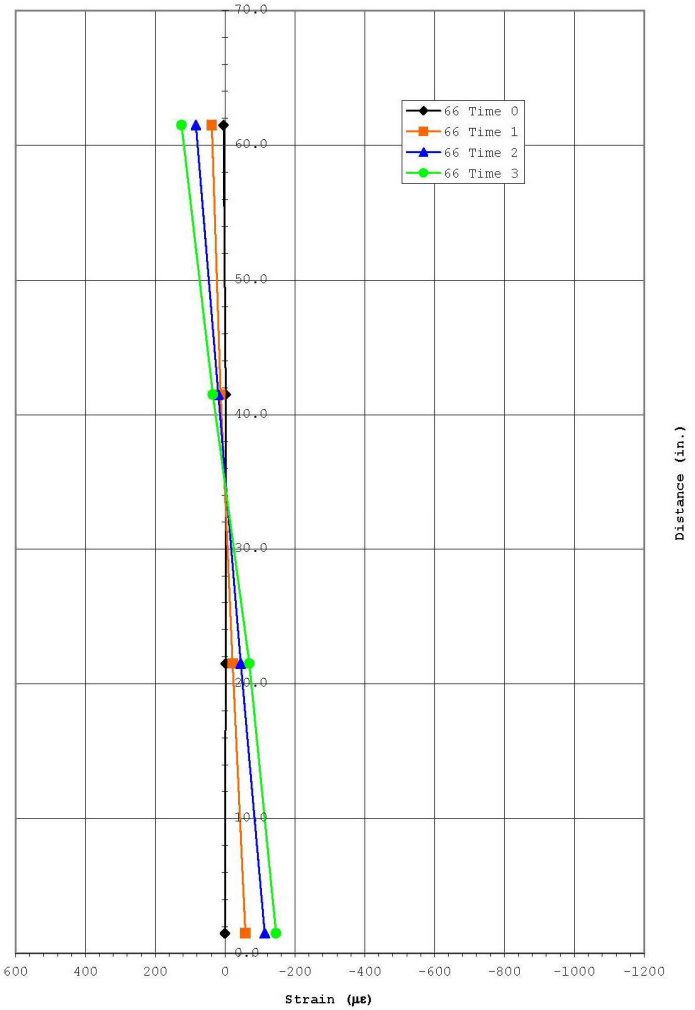

Figure A30: Strain Diagram of Station 6 on Girder 6

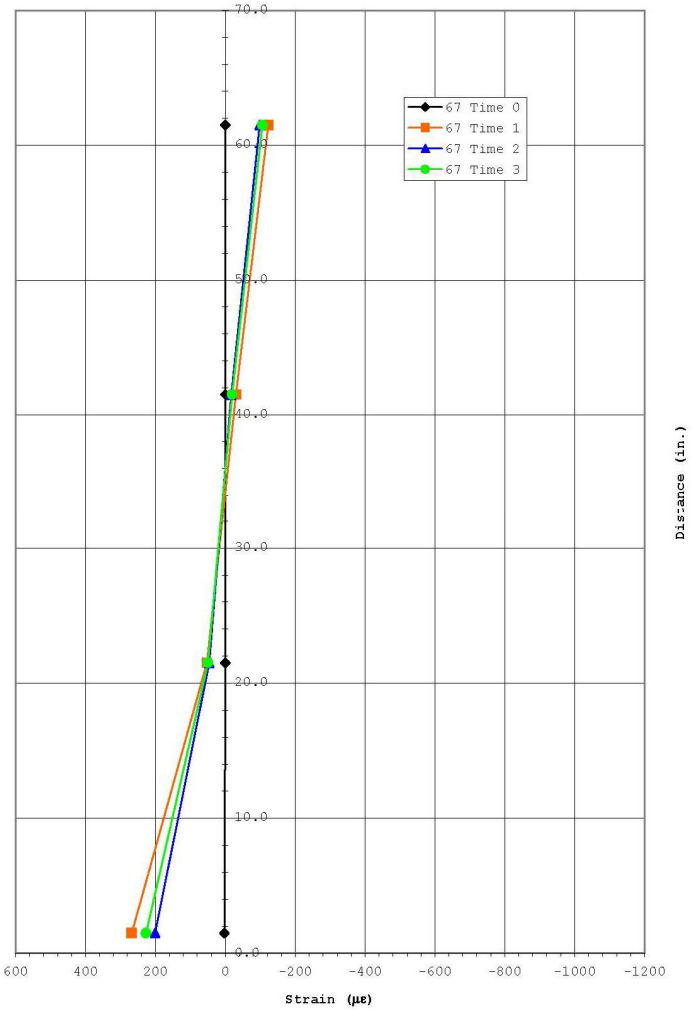

Figure A31: Strain Diagram of Station 7 on Girder 6

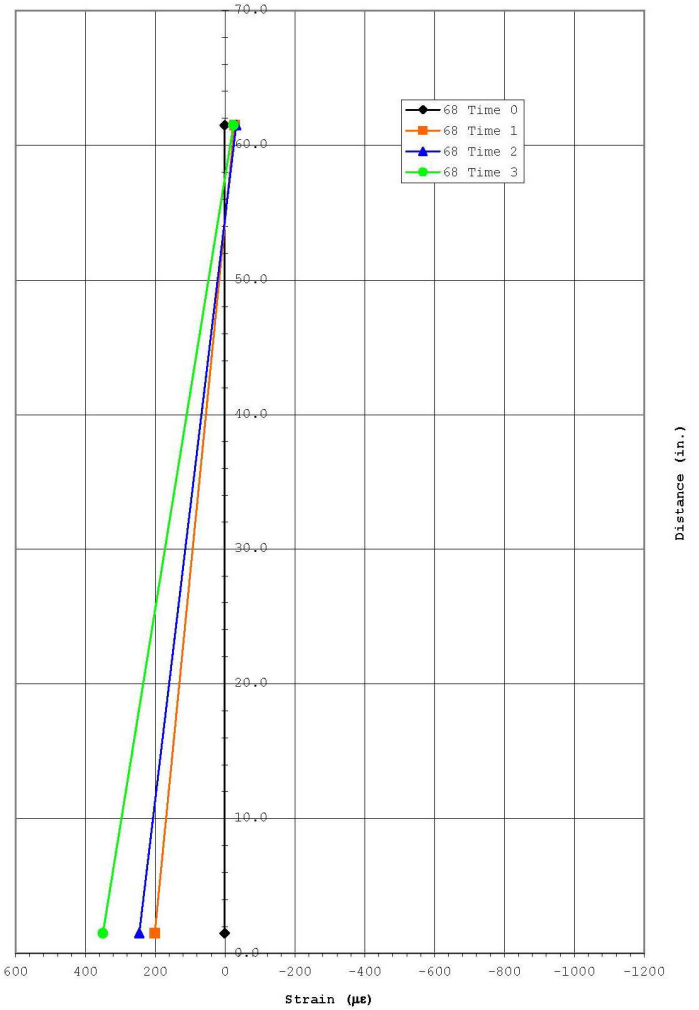

Figure A32: Strain Diagram of Station 8 on Girder 6

Figure A33: Photograph of Kicker Wedge Plates, Girders, and Diaphragm Reinforcing Steel (Kicker Wedge Plate installation is not complete)

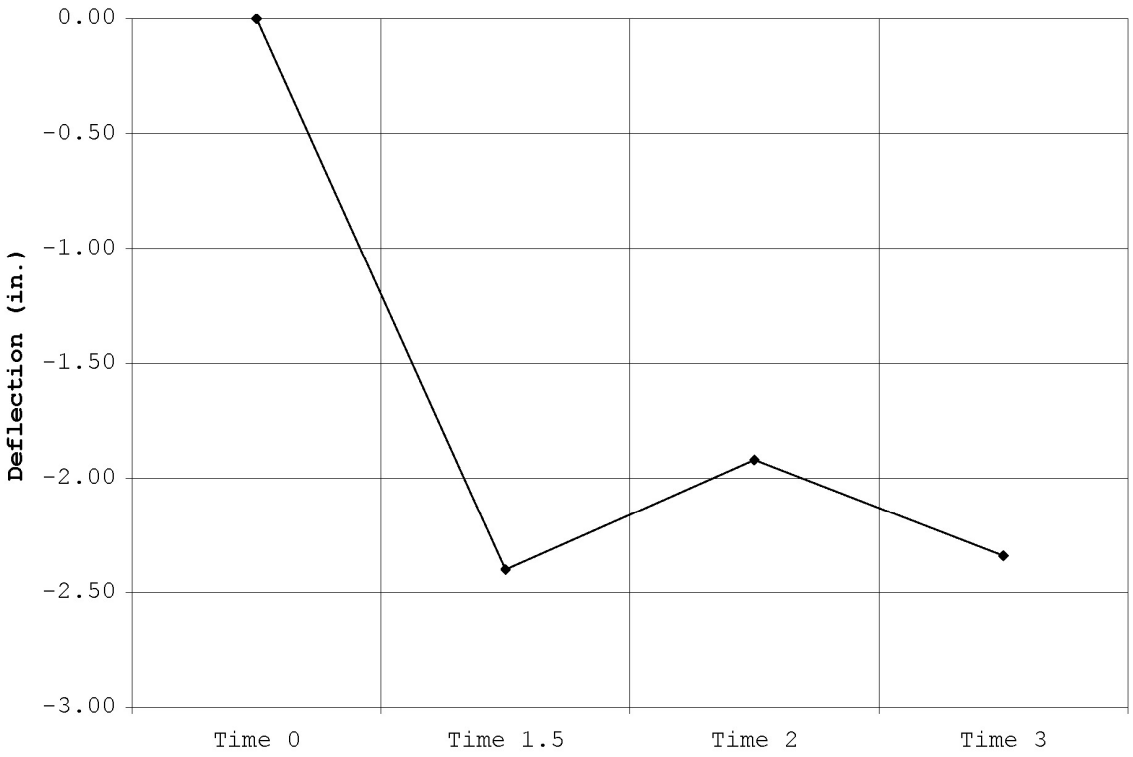

Figure A34: Girder 4 Deflections at 75ft. north of South Abutment

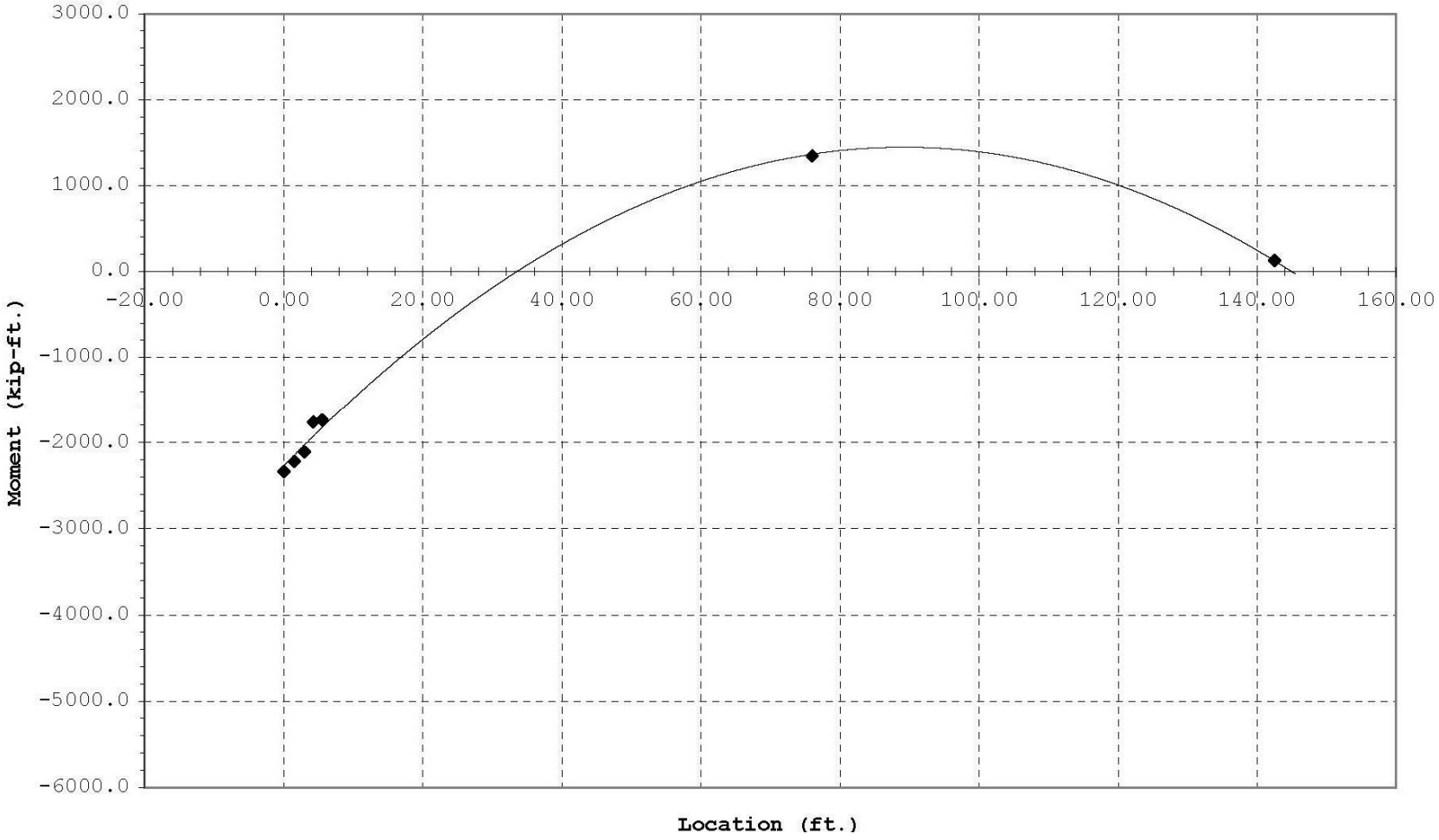

Figure A35: Moment Diagram for Measured Data along Girder 4 for Time 3

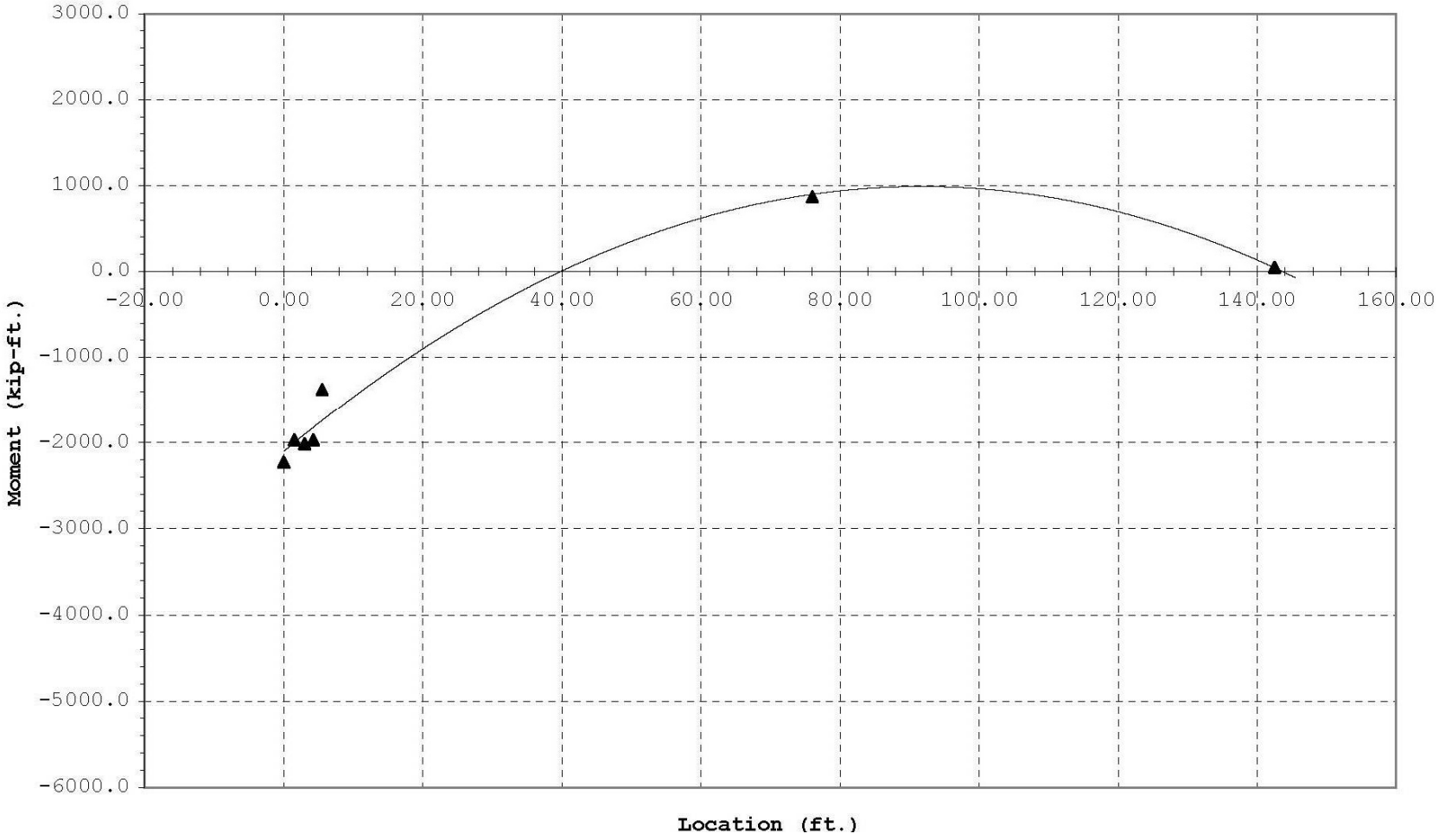

Figure A36: Moment Diagram for Measured Data along Girder 5 for Time 3

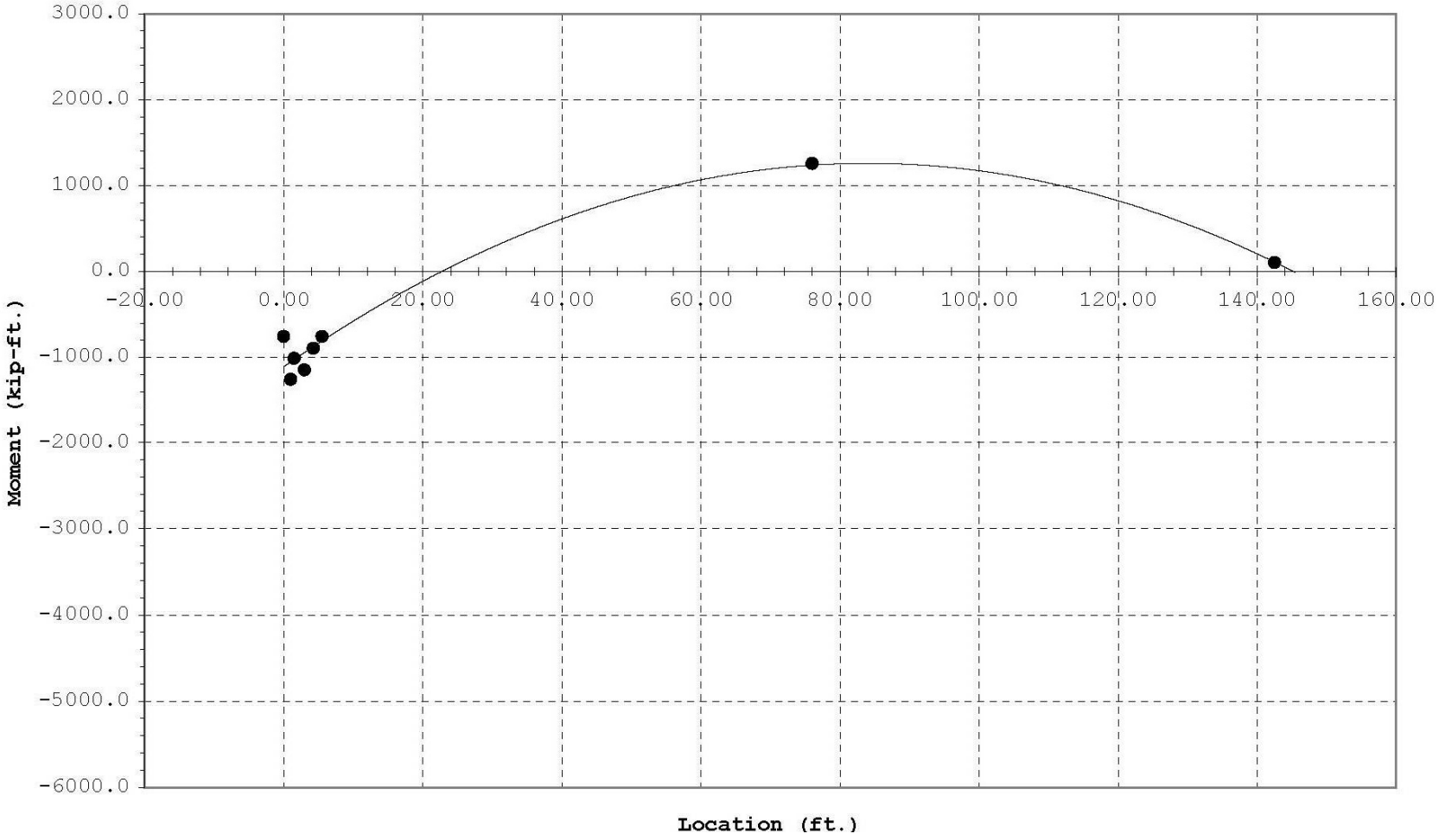

Figure A37: Moment Diagram for Measured Data along Girder 6 for Time 3

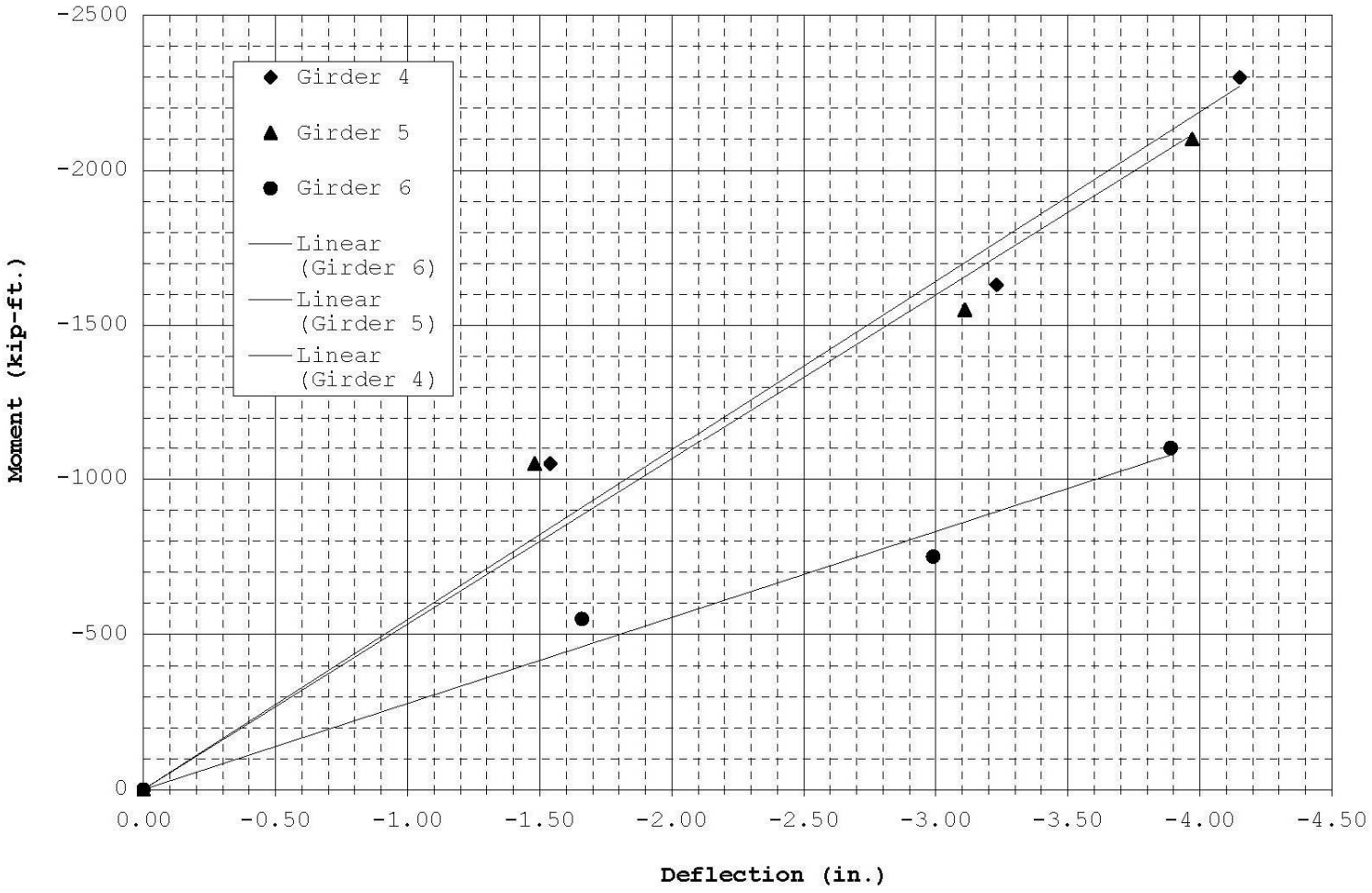

Figure A38: Moment-Deflection Diagram

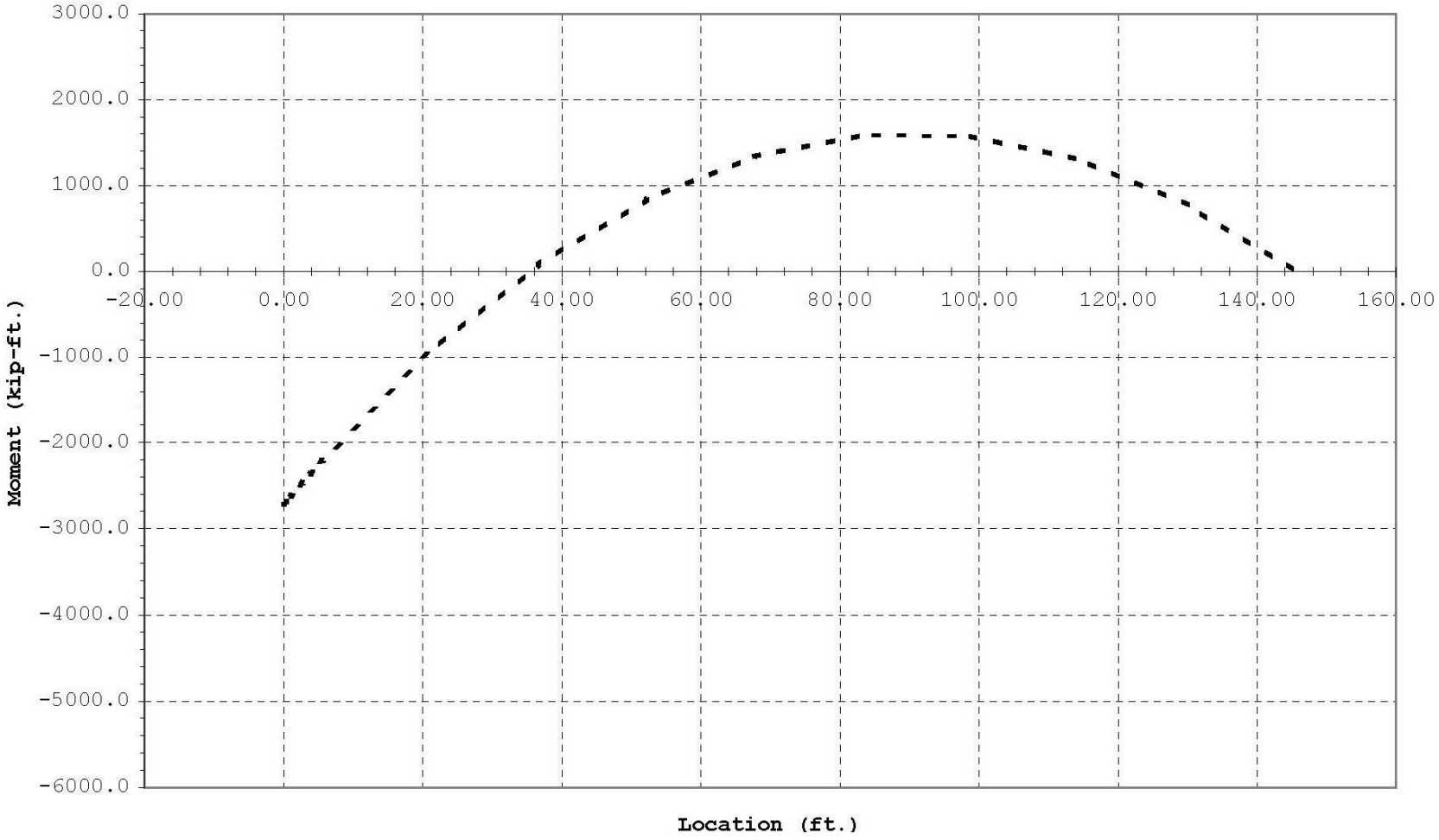

Figure A39: Theoretical Moment Diagram for Interior Girders at Time 3

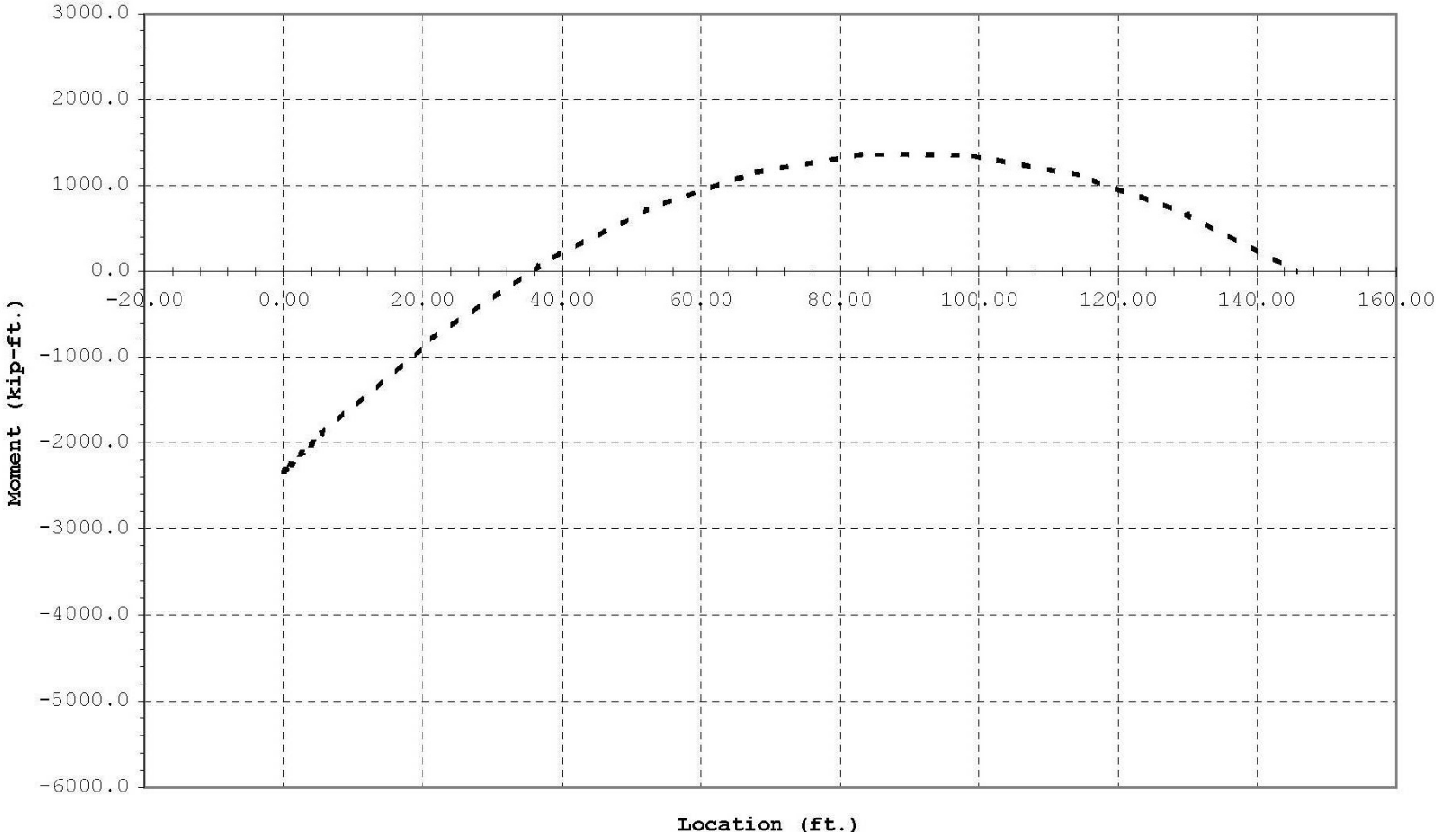

Figure A40: Theoretical Moment Diagram for Exterior Girders for Time 3

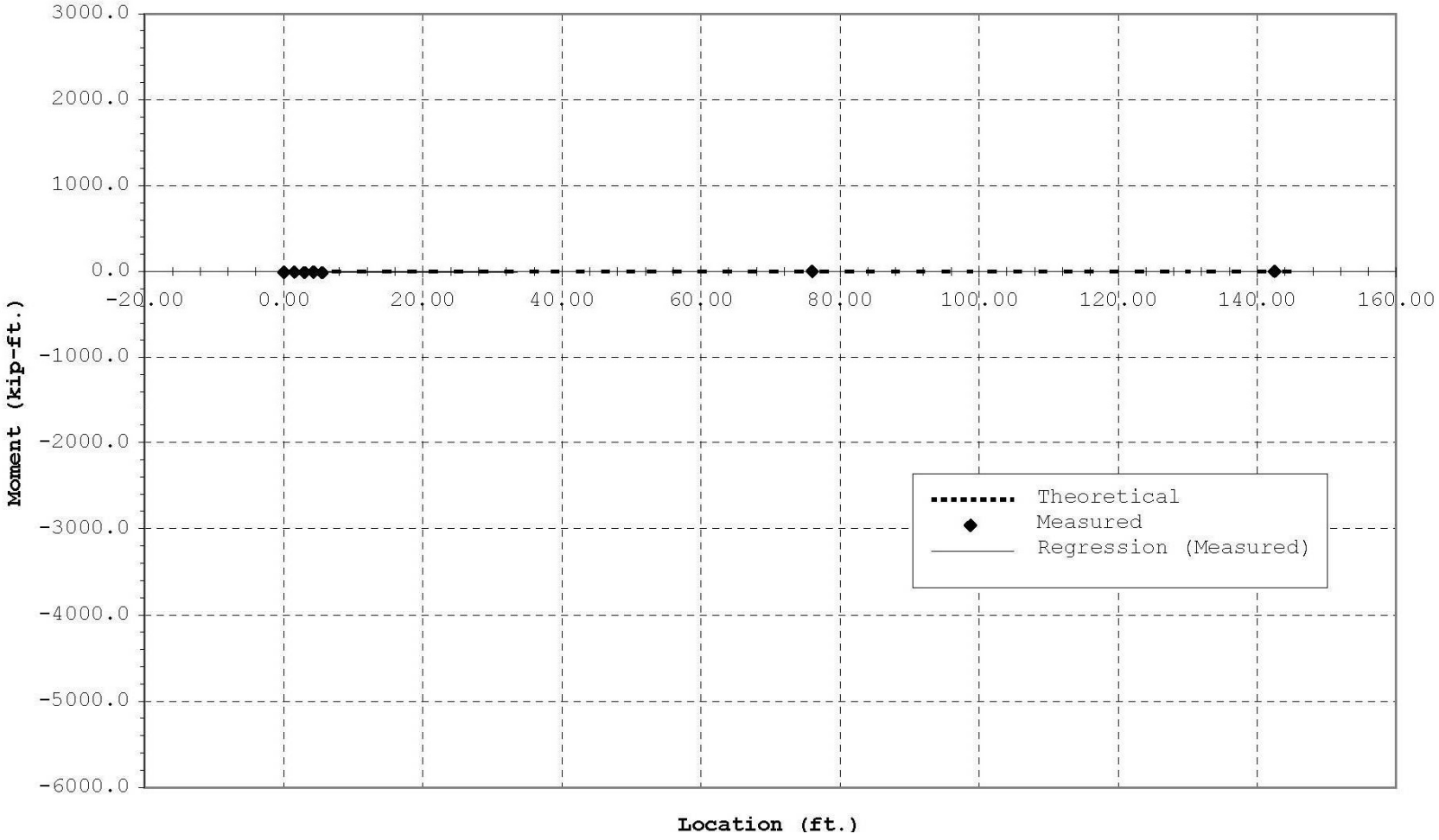

Figure A41: Theoretical and Measured Moment Diagrams for Girder 4 at Time 0

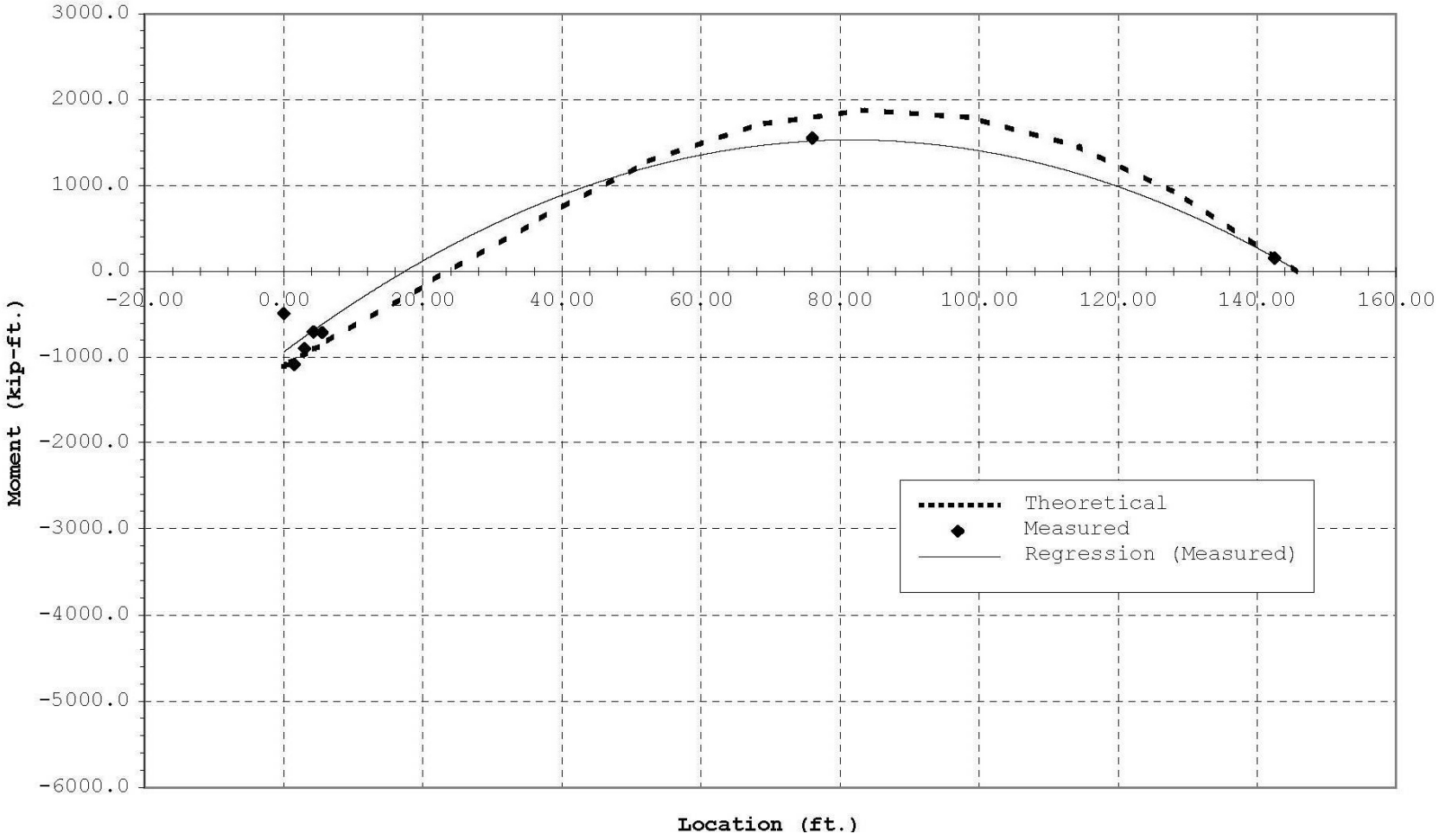

Figure A42: Theoretical and Measured Moment Diagrams for Girder 4 at Time 1

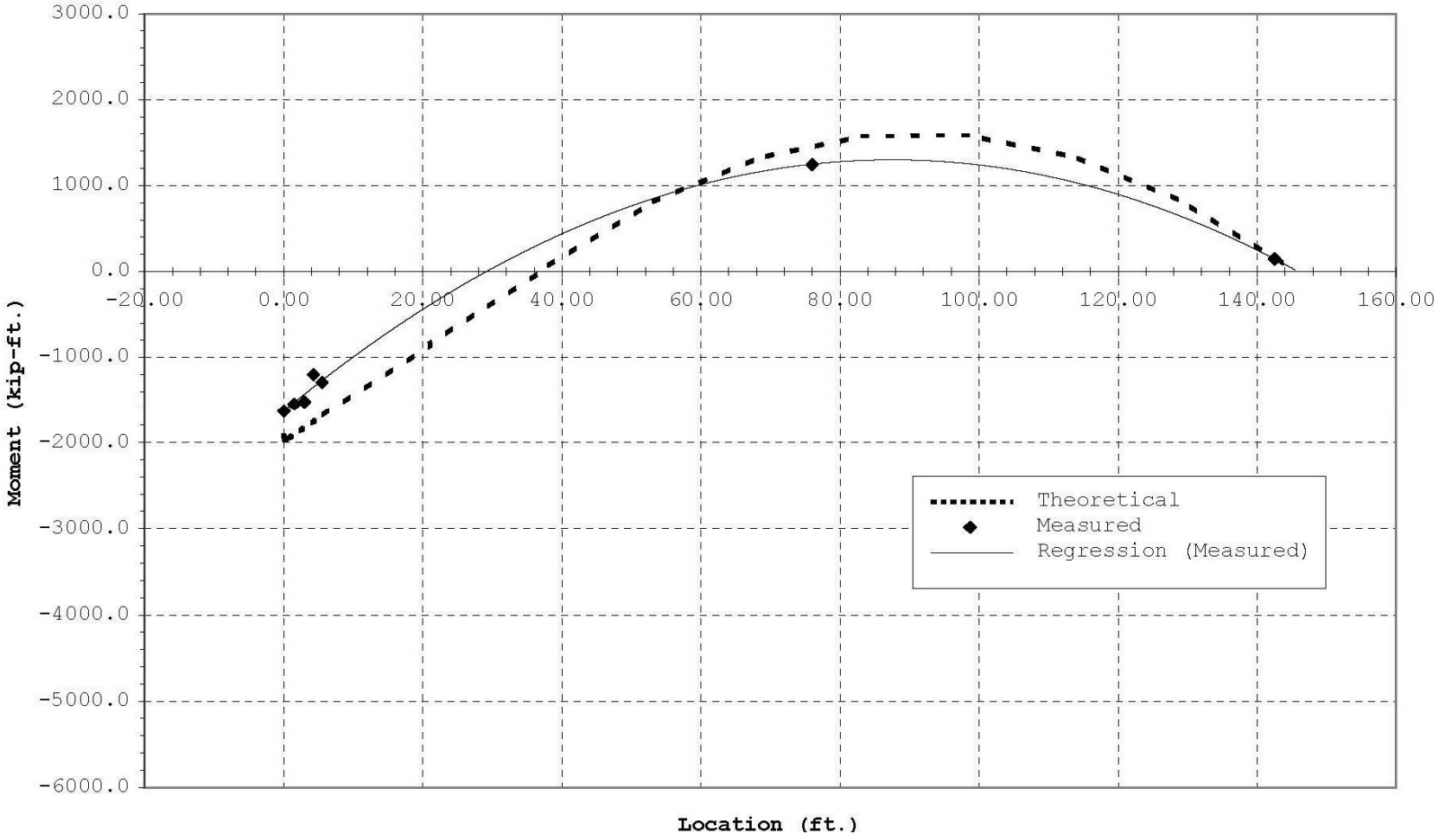

Figure A43: Theoretical and Measured Moment Diagrams for Girder 4 at Time 2

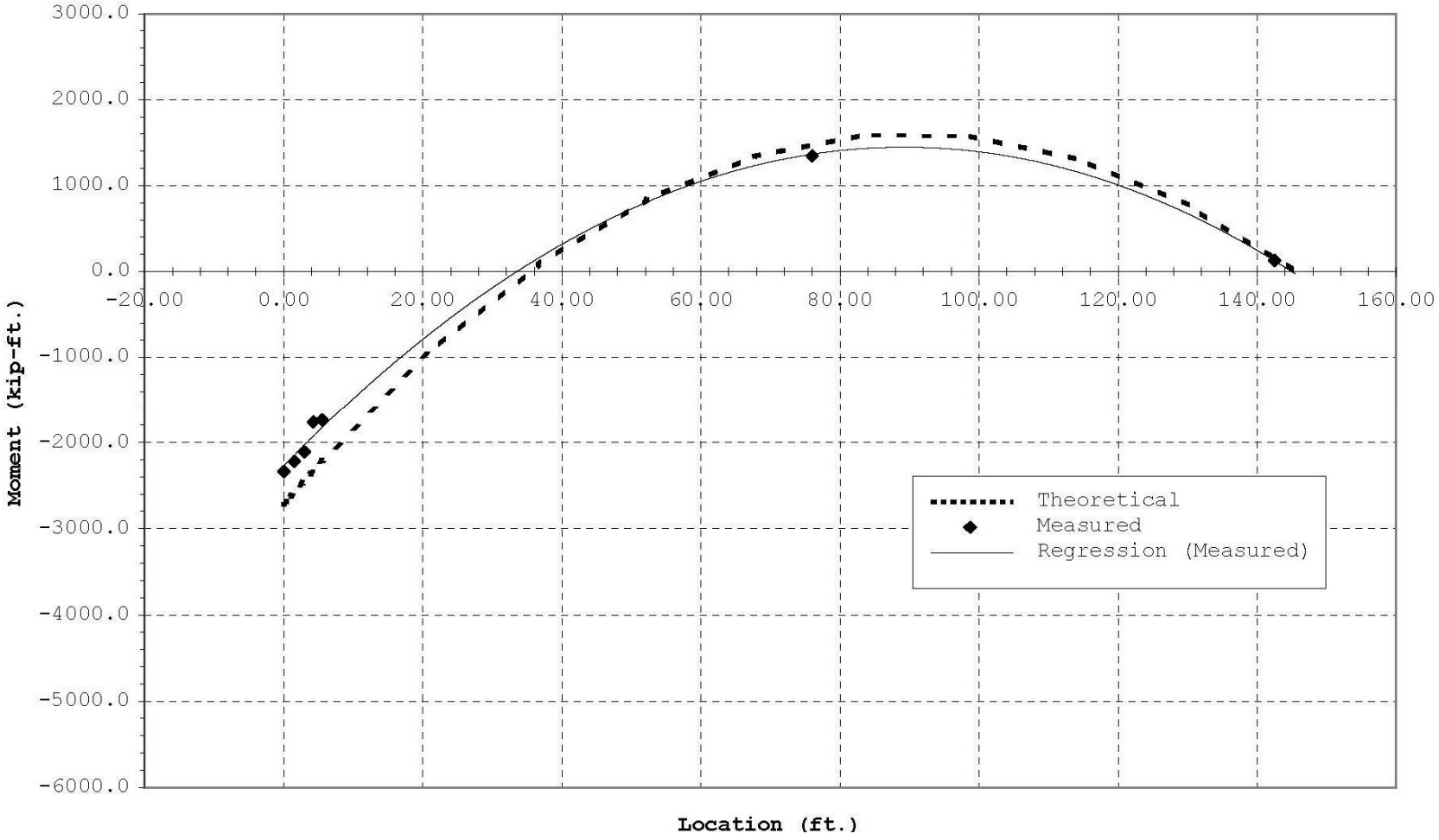

Figure A44: Theoretical and Measured Moment Diagrams for Girder 4 at Time 3

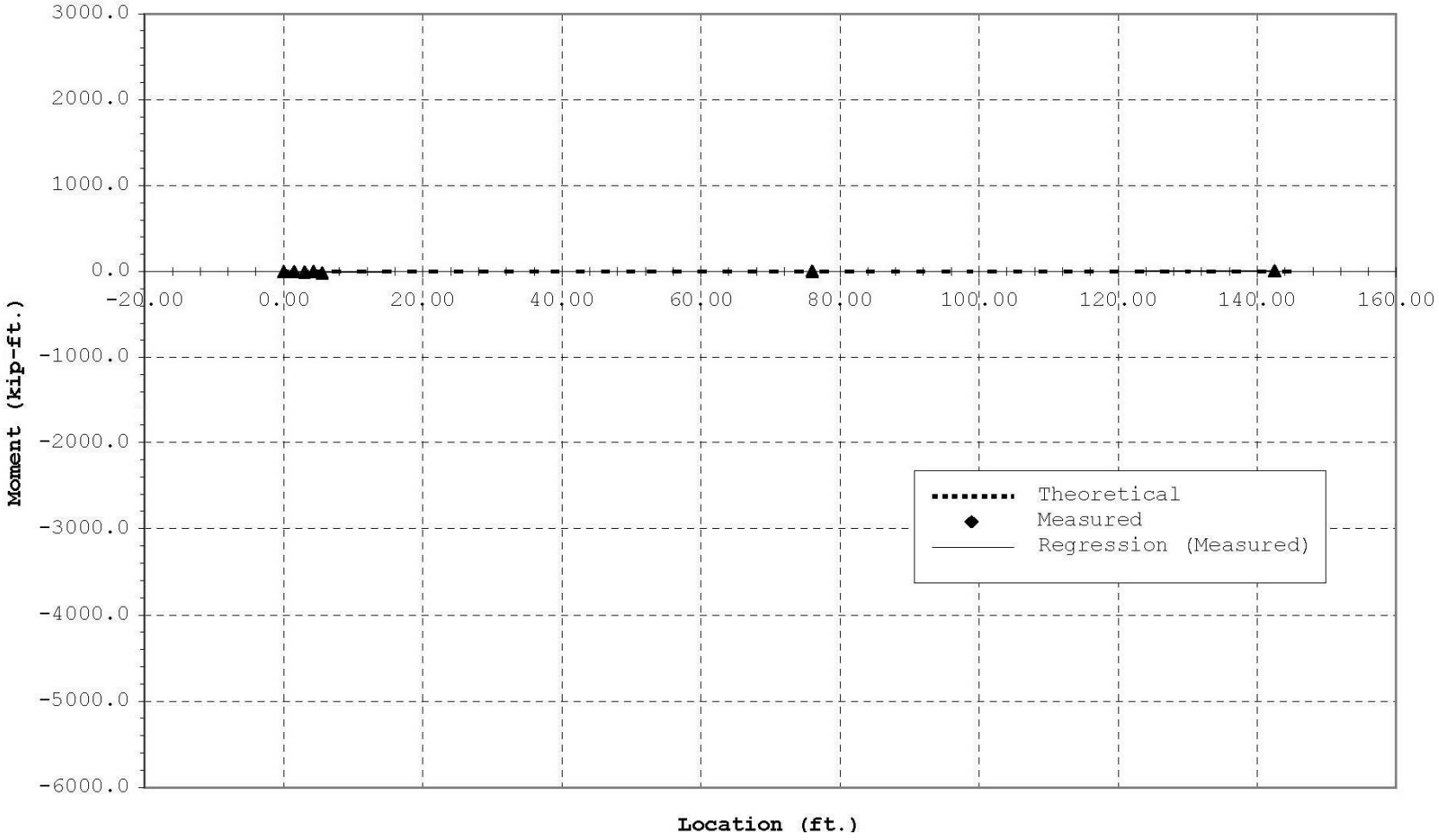

Figure A45: Theoretical and Measured Moment Diagrams for Girder 5 at Time 0

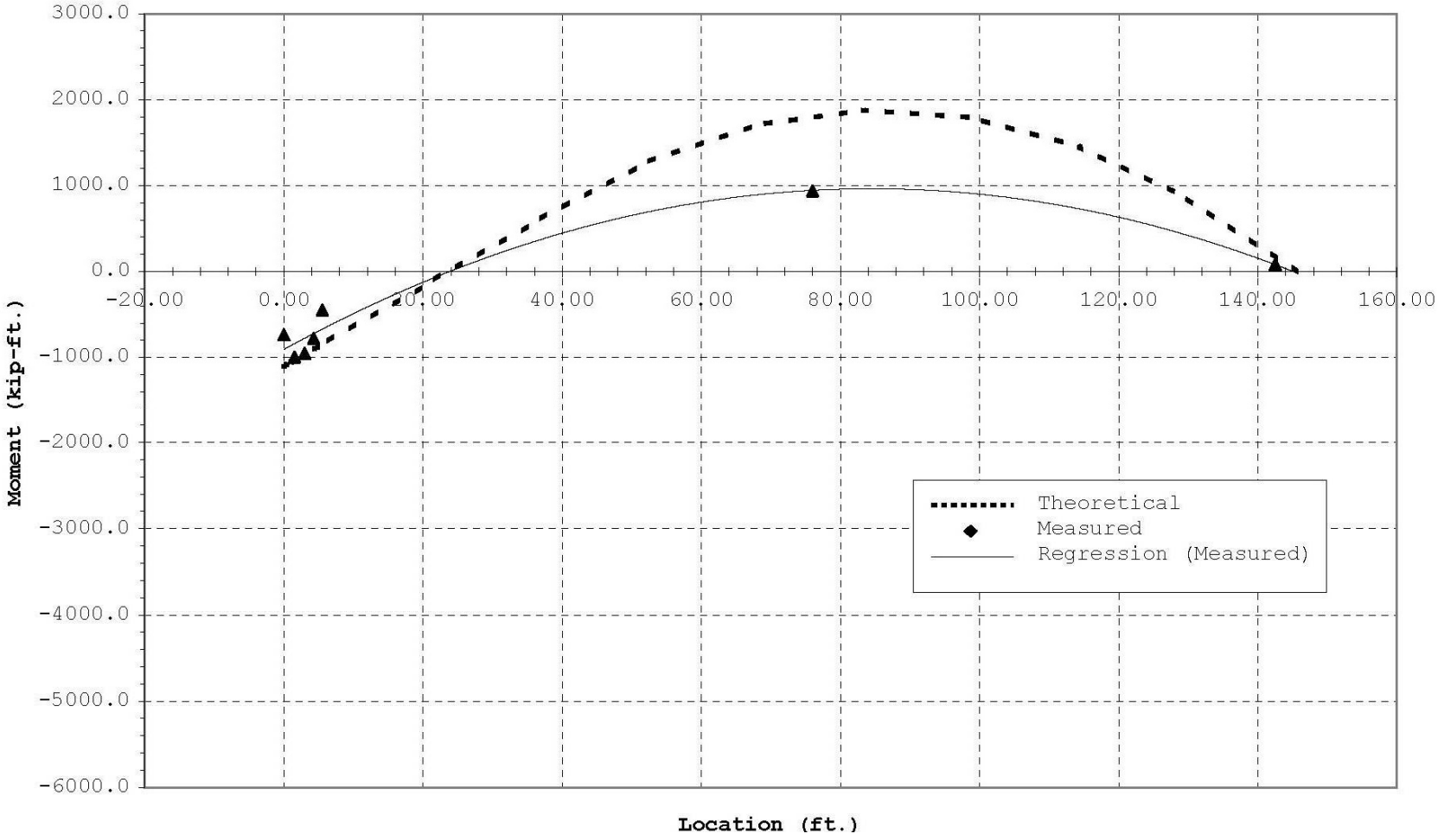

Figure A46: Theoretical and Measured Moment Diagrams for Girder 5 at Time 1

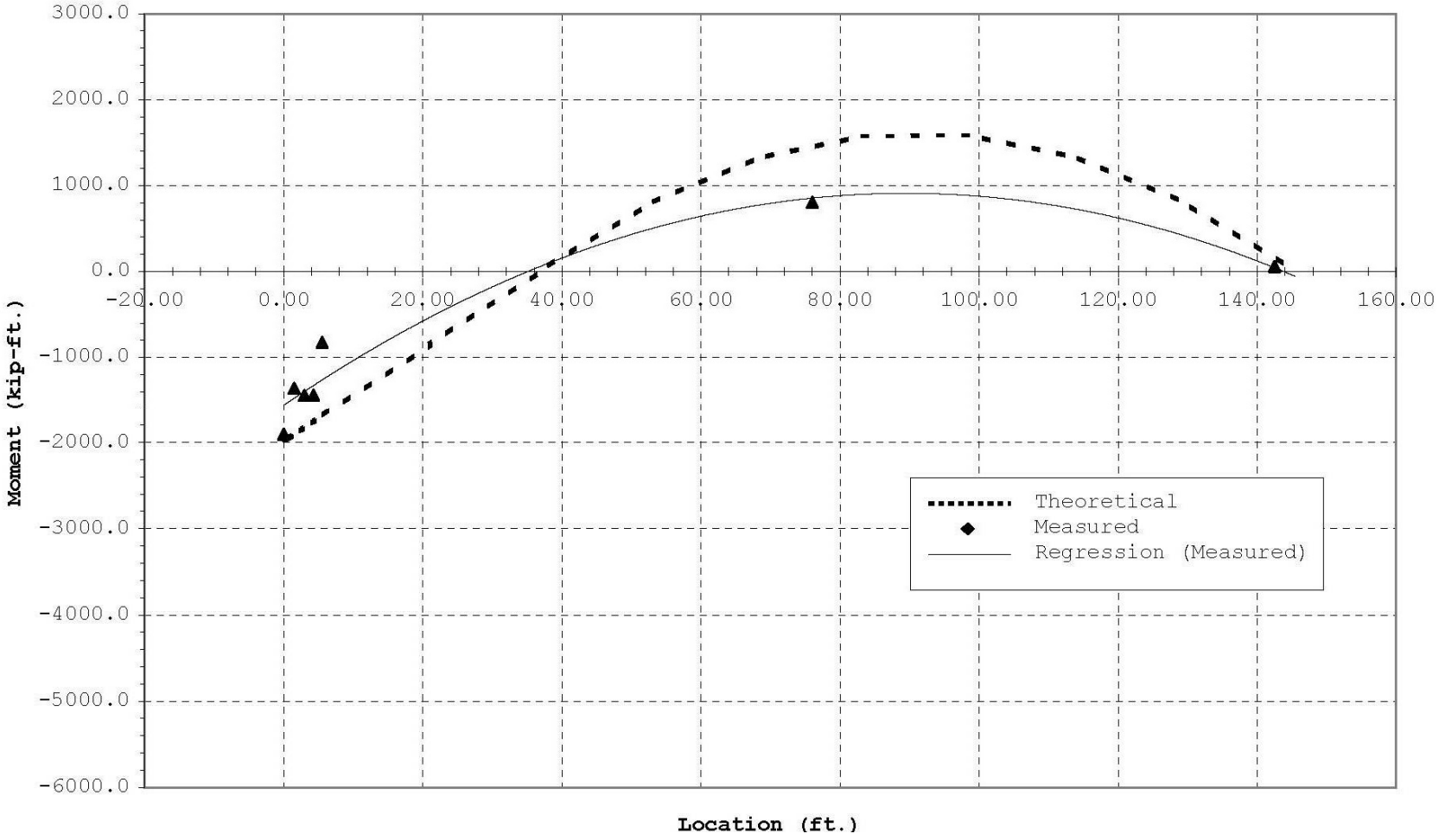

Figure A47: Theoretical and Measured Moment Diagrams for Girder 5 at Time 2

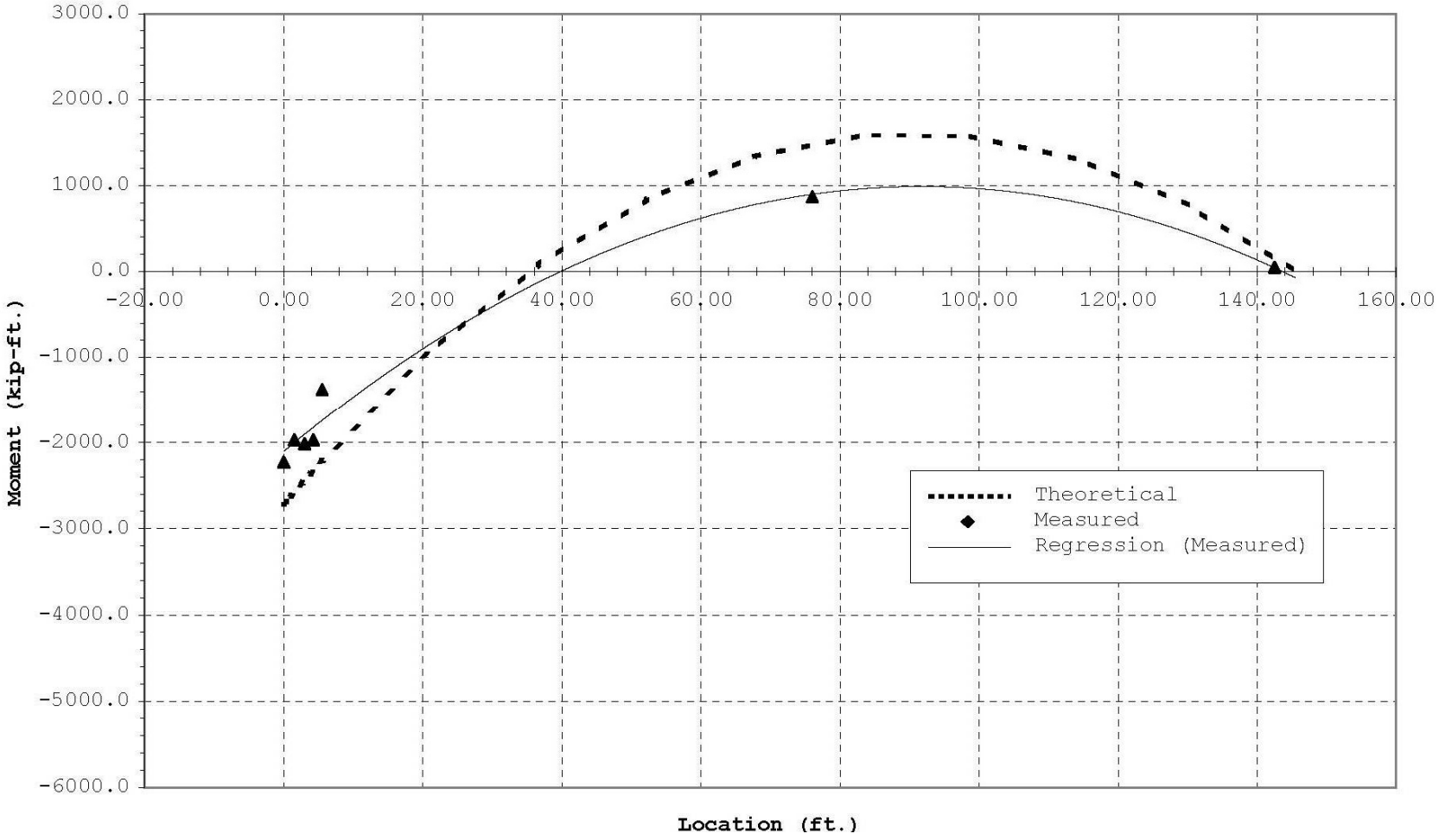

Figure A48: Theoretical and Measured Moment Diagrams for Girder 5 at Time 3

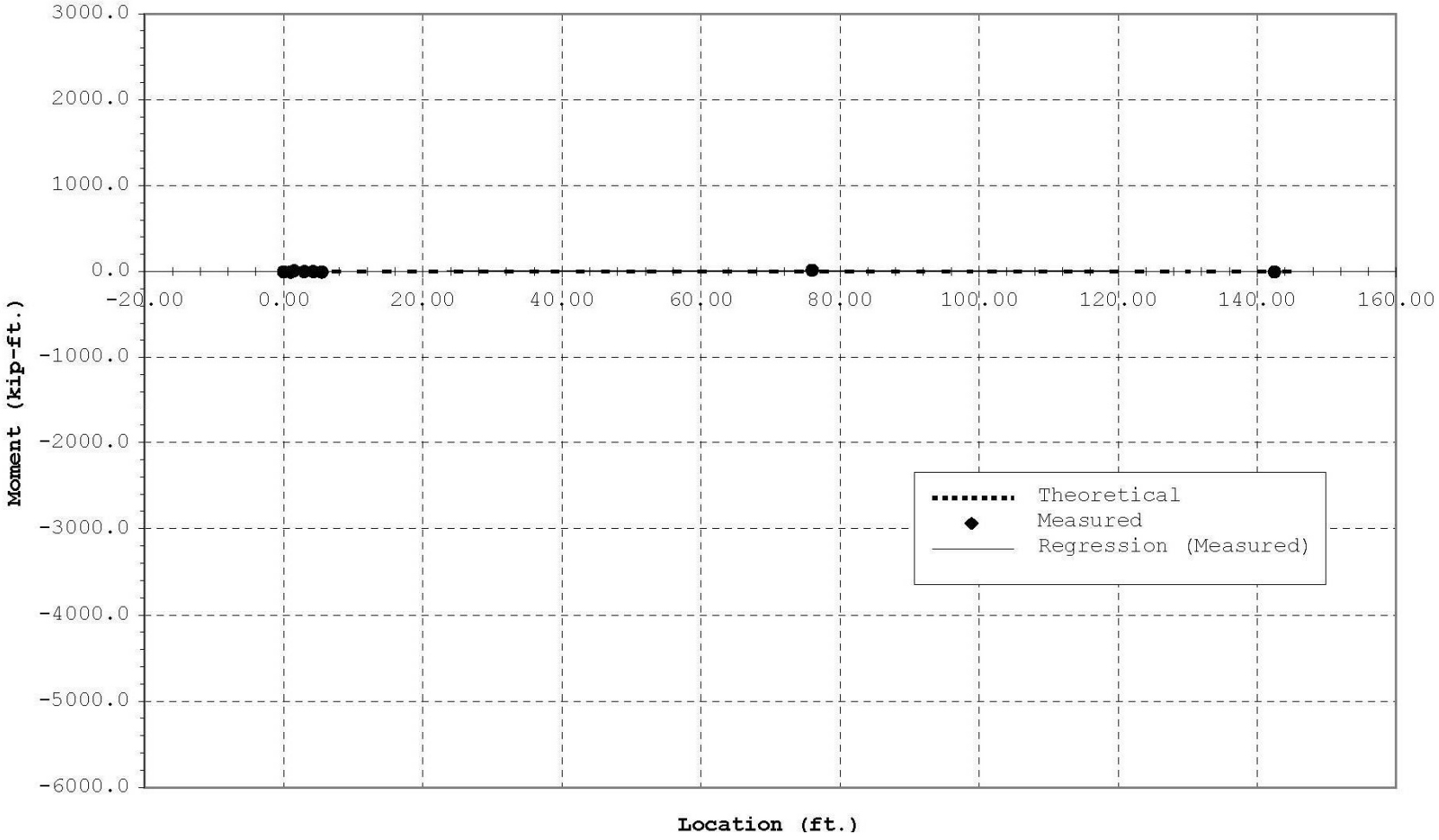

Figure A49: Theoretical and Measured Moment Diagrams for Girder 6 at Time 0

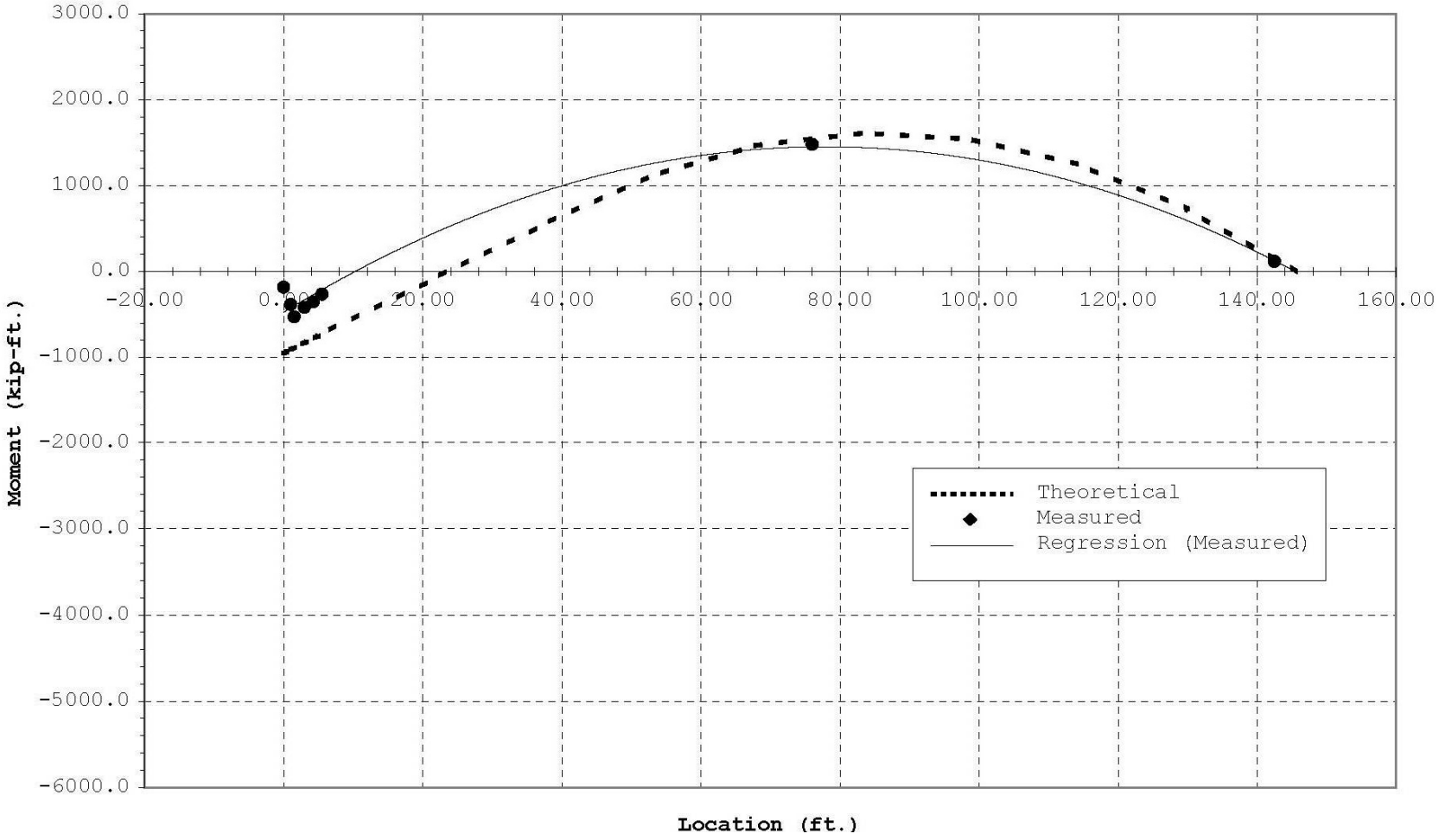

Figure A50: Theoretical and Measured Moment Diagrams for Girder 6 at Time 1

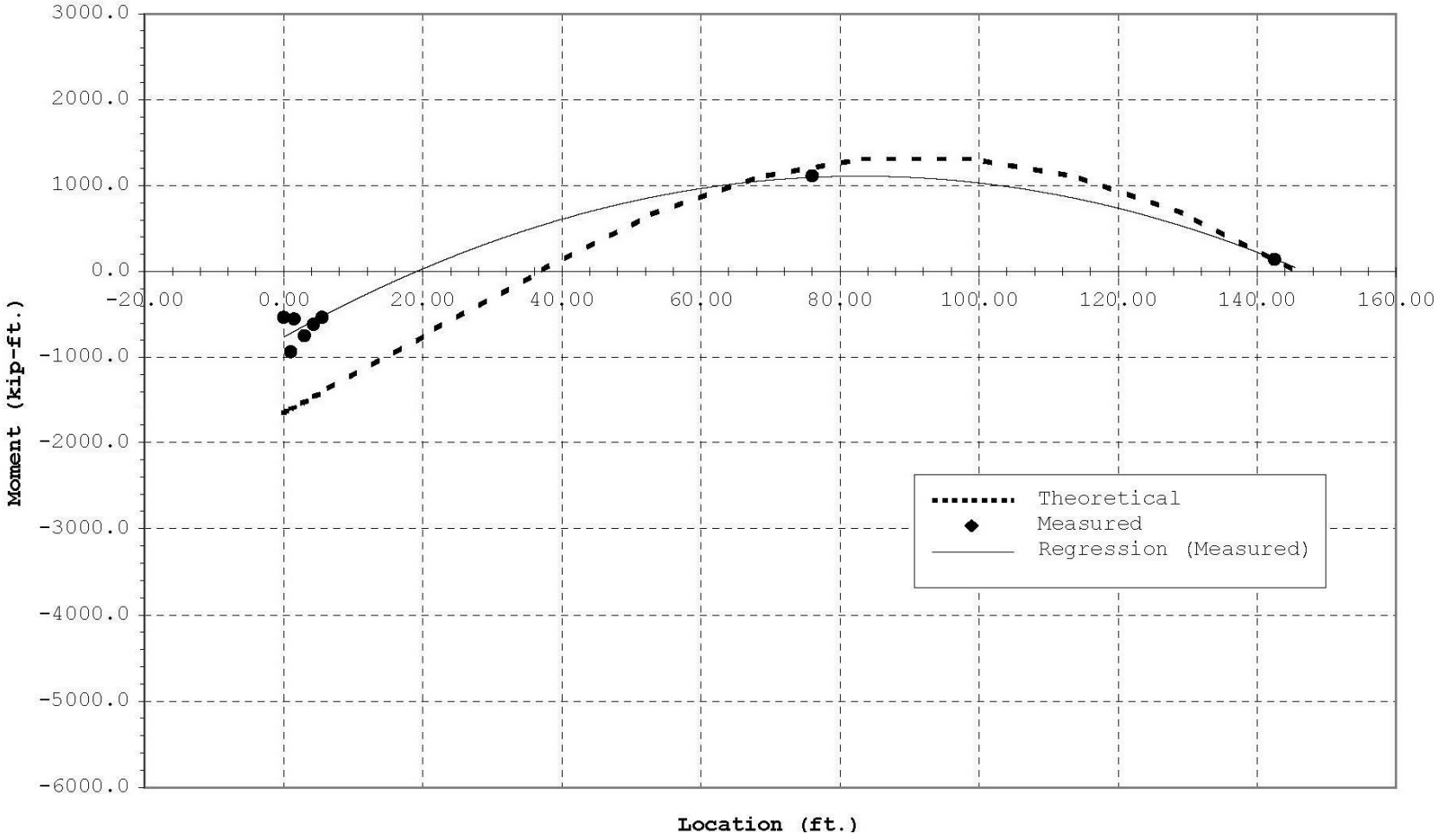

Figure A51: Theoretical and Measured Moment Diagrams for Girder 6 at Time 2

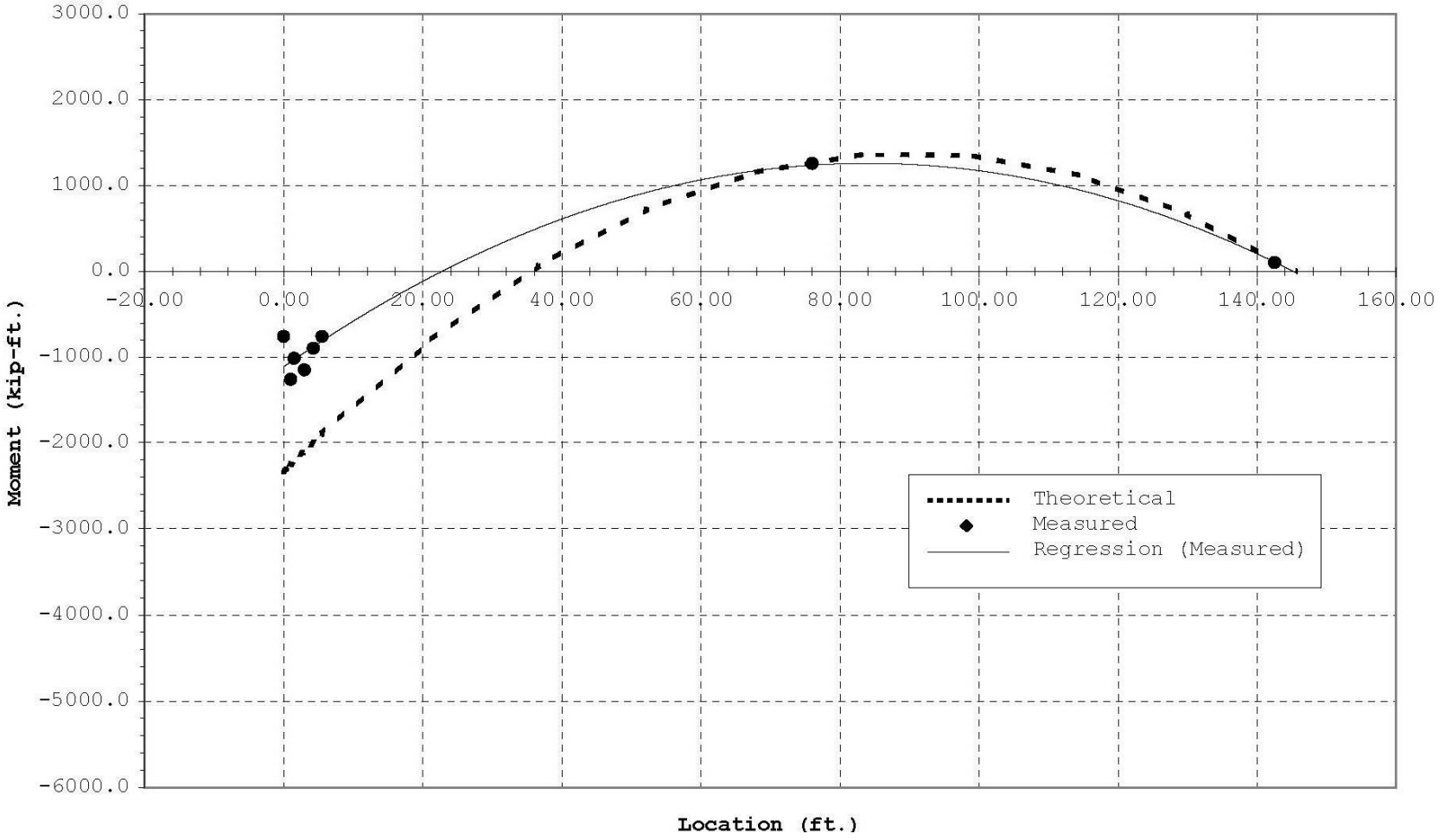

Figure A52: Theoretical and Measured Moment Diagrams for Girder 6 at Time 3

Figure A53: Photograph of Kicker Wedge Plates, Girders, and Strain Gages for Girder 6 (Kicker Wedge Plate installation is not complete)

Figure A54: Photograph of Completed Massman Drive Bridge

(View along I-40 looking west)

Vita

Jeremy Glen Pettus was born in Florence, Alabama on July 18, 1976. He was raised in Saint Joseph, Tennessee. He attended Saint Joseph Elementary School and graduated from South Lawrence Elementary School in 1990 and Loretto High School in 1994. He received the TVA Diversity Scholarship to study Nuclear Engineering at Browns Ferry Nuclear Plant (Athens, AL) provided by Chattanooga State Technical Community College (Chattanooga, TN) through an offsite degree program.

In 1996, Jeremy graduated cum laude with an A.S. in Nuclear Engineering Technology from Chattanooga State Technical Community College (Chattanooga, TN). That same year, he enrolled into the undergraduate physics program at the University of North Alabama (Florence, AL). In 1998, he graduated magna cum laude from the University of North Alabama (Florence, AL) with a B.S. in Professional Physics with a minor in Mathematics. He received a graduate teaching assistantship through the Department of Physics and Astronomy at the University of Tennessee (Knoxville, TN).

In 2000, Jeremy graduated summa cum laude with a B.S. in Civil Engineering from the University of Tennessee (Knoxville, TN).

In 2001, Jeremy worked as a structural engineer (intern) with Bigbee Steel Buildings, Inc. (Muscle Shoals, AL) until being employed with TTL, Inc. (Tuscaloosa, AL) as a geotechnical engineer (intern). He was transferred to the TTL, Inc. (Decatur, AL) office in July 2002. In 2004, he received a graduate teaching assistantship, a graduate research assistantship, and the Dr. Edwin G. and Patsy Burdette Graduate Fellowship through the Civil and Environmental Engineering Department at the University of Tennessee (Knoxville, TN).

Jeremy began his studies in August, 2004 and received his M.S. in Civil Engineering, Structural Concentration, in August, 2005. Upon graduation, he was employed by the Tennessee Valley Authority (Chattanooga, TN) in the Transmission Line Engineering Division.